



# Combining microbial, isotopic and residence time data to characterize groundwater dynamics in a multi-layered aquifer system in Kurikka, western Finland

Lotta Purkamo<sup>1</sup>, Juuso Ikonen<sup>1</sup>, Marie-Amélie Pétré<sup>1,a</sup>, Niko Putkinen<sup>1</sup>, Jürgen Sültenfuss<sup>2</sup>, Minna Myllyperkiö<sup>1</sup>, Anna-Maria Hokajärvi<sup>3</sup>, Tarja Pitkänen<sup>3,4</sup>, and Ilkka T. Miettinen<sup>3</sup>

<sup>1</sup>Geological Survey of Finland (GTK), Espoo, 02150, Finland

<sup>2</sup>University of Bremen, Otto Hahn Allee 1, 28359 Bremen, Germany

<sup>3</sup>Finnish Institute for Health and Welfare (THL), Department of Public Health, Kuopio, 70210, Finland

<sup>4</sup>University of Helsinki, Faculty of Veterinary Medicine, Helsinki, 00014, Finland

<sup>a</sup>current address: BRGM – French Geological Survey, 45060 Orléans, France

**Correspondence:** Lotta Purkamo (lotta.purkamo@gtk.fi)

Received: 26 September 2025 – Discussion started: 22 October 2025

Revised: 22 May 2026 – Accepted: 28 May 2026 – Published: 6 July 2026

**Abstract.** Groundwater is a critical resource supplying nearly half of the world's drinking water. This study focuses on the Kurikka buried valley aquifer system in western Finland, characterized by complex hydrogeology dictated by the bedrock topography and sediment cover producing artesian conditions in deep aquifers. Using a multitracer approach, the study incorporates hydrogeochemical, isotopic ( $\delta^2\text{H}$ ,  $\delta^{18}\text{O}$ ,  $\delta^{34}\text{S}$ ,  $^{87}\text{Sr}/^{86}\text{Sr}$ ) and microbial community analyses with residence time indicators (CFCs,  $\text{SF}_6$ ,  $^3\text{H}$ ,  $^3\text{H}/^3\text{He}$ ). Groundwater samples collected from ten sites revealed differences in residence times, microbial diversity and community compositions, as well as large variation in the strontium and sulphur isotopic compositions. The bedrock groundwater sample revealed a more evolved water type, consistent with longer residence time, strong water-mineral interactions and typical deep subsurface bacterial members. Groundwater from the superficial unconsolidated aquifers contained a modern water component ( $< 60$  years) whereas the deeper buried valley aquifers were characterized by older waters. The information provided by this study is crucial for groundwater management during extensive extraction for municipal water supply.

## 1 Introduction

Groundwater provides an essential water supply worldwide. Almost half of all drinking water globally, 65 %–75 % in Europe (27 EU Member States) and 38 % in the US (Grönwall and Danert, 2020; Johnson et al., 2022, National Ground Water Association, 2025) originates from groundwater. In Finland, approximately 60 % of water distributed by waterworks is groundwater and the management of groundwater resources is crucial to the success of the water utilities producing good quality drinking water (Kløve et al., 2017). To manage the groundwater resources sustainably, a significant understanding of the aquifer is essential. Hydrogeochemical investigations play a key role in characterizing hydrogeological systems and are commonly supported by multitracer approaches that integrate major ions, trace elements, stable water isotopes, and environmental tracers. Such approaches are widely used to constrain groundwater origin, flow paths, residence times, mixing and water/rock interactions (Cloutier et al., 2006; Jaunat et al., 2012; Pétré et al., 2016). However, despite the proven value of conventional hydrogeochemical tracers, uncertainties often remain in complex multiaquifer systems regarding hydraulic connectivity, inter-aquifer mixing, and interactions between unconsolidated sediments and fractured bedrock groundwater. These uncertainties can limit the ability to predict groundwater flow dynamics and sustainably manage groundwater abstraction.

Buried valley aquifer systems are particularly challenging to characterize due to their complex geometry and heterogeneous sedimentary architecture. This is also the case in Kurikka, western Finland: the aquifer system investigated in this study hosts significant groundwater resources. The aquifer system has a complex groundwater recharge route originating from the high-standing areas west of the Kurikka buried valleys. From the recharge area, groundwater flows toward the buried valley aquifers, where the lowermost coarse-grained aquifer consists of the interplay between permeable sediments and fractured crystalline bedrock (Åberg et al., 2026). Despite previous hydrogeological investigations, flow paths and the degree of mixing between shallow (here up to 70 m) and deeper sediments (70–120 m) and the bedrock groundwater remain poorly understood, constituting a key knowledge gap for sustainable groundwater management in the area. To address these challenges, this study applies an expanded multitracer approach that integrates hydrogeochemical, isotopic, and groundwater age tracers, complemented with microbial community analyses.

Stable water isotopes of hydrogen ( $\delta^2\text{H}$ ) and oxygen ( $\delta^{18}\text{O}$ ) are used to assess groundwater origin, recharge conditions and mixing processes (e.g., Åberg et al., 2025; Carreira and Marques, 2024; Ikonen et al., 2025; Luoma et al., 2024), while the measurement of strontium isotopes is used to determine the  $^{87}\text{Sr}/^{86}\text{Sr}$  ratio providing additional information about the water-rock interaction and source lithology (Kaislaniemi, 2011; Shand et al., 2009). Sulfur isotope composition, expressed as  $\delta^{34}\text{S}$ , is commonly used as a tracer of sulfur sources and associated biogeochemical processes in groundwater systems reflecting specifically the biogeochemical processes (Harrison and Thode, 1958; Kaplan and Rittenberg, 1964; Onac et al., 2011; Samborska-Goik and Bottrell, 2025) and is applied here as an additional isotopic tracer. Groundwater residence times and flow dynamics are evaluated using a suite of environmental tracers, including tritium ( $^3\text{H}$ ), chlorofluorocarbons (CFCs), sulfur hexafluoride ( $\text{SF}_6$ ) and noble gases. These tracers are useful because of their known input histories or predictable decay or accumulation in the subsurface, and have been widely applied across a range of hydrogeological contexts, including in bedrock aquifers (Åkesson et al., 2015; Cook and Solomon, 1997; Jaunat et al., 2012; Massmann et al., 2008; Mayer et al., 2014; Meyzonnat et al., 2023; Osenbrück et al., 2006; Visser et al., 2013).

Although multitracer hydrogeochemical approaches are well established in hydrogeology, microbial information is still only rarely integrated into aquifer characterization studies. In recent years, microbial community analyses have emerged as a promising complementary tool for hydrogeology, with the potential to reflect subsurface conditions, hydraulic connectivity and geochemical environments (Ben Maamar et al., 2015). Groundwater as a dark and often oligotrophic environment with relatively stable temperature selects specific microbial communities compared to the aquatic

ecosystems aboveground (Lee et al., 2018). Although advances in molecular biological methods have greatly improved the characterisation of groundwater microbial diversity, microbial community structure remains to be fully exploited in understanding the hydraulic connections in aquifers (Merino et al., 2022). Integrating microbial data with hydrogeochemical and isotopic tracers may therefore provide novel insight into aquifer functioning.

This study forms part of a larger hydrogeological research initiative, aimed at securing sufficient groundwater resources to support large-scale abstraction to meet the water demands of 150 000 residents and the industries in cities of Vaasa and Kurikka. The overarching objective of this study is to establish baseline hydrogeochemical and microbiological conditions that enable the monitoring of the evolution of the water system during operational stage of abstraction. Specifically, the research addresses the question of whether a combined multitracer hydrogeochemical and microbial community analysis approach improves the characterisation of groundwater origin, residence time, flow paths and connectivity in a complex buried valley aquifer system. We hypothesize that this multitracer approach in hydrogeochemistry combined with lesser used microbial community analysis provides additional constraints on groundwater connectivity and flow dynamics within complex multi-aquifer systems. Such information is critical for informed decisions about groundwater management and sustainable resource development.

### Site description

The study site is situated in the Southern Ostrobothnia region in western Finland, 70 km from the Bothnian Sea shore (Fig. 1). The groundwater system of the Kurikka buried valley is underlain by 1.88 Ga year-old Palaeoproterozoic metamorphosed granites, schists, and biotite paragneisses (Lahtinen et al., 2017; Ruuska et al., 2023). The early development of the Paleoproterozoic bedrock during the Svecofennian orogeny with crustal movements, shaped the Kurikka area and led to the formation of protovalleys. Since then, the area has experienced a multi-stage burial-erosion development over a long period of time until it reached its current buried form (Hall et al., 2021). Currently, this  $\sim 1.5$  Ga old and 70–120 m deep buried valley system is filled with highly variable Late Pleistocene sediments. In its most recent developmental stages, this region situated beneath the central sector of the Fennoscandian Ice Sheet (FIS) during the Late Weichselian Glaciation (23 000–10 500 years BP; Stroeven et al., 2016) – which covered southern Finland and facilitated the preservation of pre-existing sediments through limited glacial erosion (Åberg et al., 2026) – remained largely unaffected. Specifically, the deepest sediments typically consist of deposits that have groundwater potential for municipal drinking water abstraction.

The regional hydrogeology of the study area (240.5 km<sup>2</sup>, Fig. 1) is strongly controlled by bedrock topography. Topographical differences, together with silt-clay sediment and basal till on the topmost part of the sediment cover, produce an artesian character to the deep aquifers (Fig. 1). Deep groundwater in the unconsolidated aquifers in the Kurikka aquifer system translates to a maximum depth of about 120 m from the land surface (Åberg et al., 2026). Groundwater in Finland mainly resides in shallow unconfined aquifers (Lahermo et al., 1990; Luoma et al., 2021), and the deepest aquifer in the multi-layered system in Kurikka is nominated deep in this context. Layer cake type of stratigraphy of the buried valley with alternating aquitards and aquifers is conceptually shown in the Fig. 1, but more detailed in Åberg et al. (2026).

## 2 Materials and Methods

In this multi-tracer study of the region, the sampling points were selected in each buried valley connected to the main Kyrönjoki Valley (Fig. 1). Additionally, the study included a bedrock borehole (R56) located beneath the Paloluoma valley and a point further north (NOPPA15) in an adjacent valley reflecting a more superficial esker system.

### 2.1 Field parameter measurements, geochemical and isotope sampling and analyses

The water samples were collected between 4 and 7 October in 2021. The groundwater wells (apart from those that were overflowing) were purged 1 d before sampling. The water levels were measured at non-overflowing wells before sampling. Groundwater was pumped from the wells using a submersible pump (Proactive SS-Monsoon XL, GWM Engineering, Kuopio, Finland) with pumping speed of 4–7 L min<sup>-1</sup>. The field measurements for temperature (T), dissolved oxygen (DO), pH, electrical conductivity (EC) and oxygen reduction potential (ORP) were recorded with YSI multi-parameter sonde (YSI EXO1) (YSI Inc. Yellow Springs, OH, US). Alkalinity was measured in the field with a HACH digital titrator (HACH Company, Loveland, CO, US) and a cartridge of sulphuric acid (1.600 N). The partial pressure of CO<sub>2</sub> (*p*CO<sub>2</sub>) was calculated with the software Diagrammes (Simler 2012) based on temperature, pH and HCO<sub>3</sub> concentration. For hierarchical clustering, selected parameters (pH, EC, *T*, DO and alkalinity) were used for calculating Euclidean distance matrix, and clustering was done with UPGMA (Unweighted Pair Group Method with Arithmetic Mean) method in R with *vegan*, *ggplot2* and *ggdendro* packages (Oksanen et al., 2025; de Vries and Ripley, 2024; Wickham et al., 2026). Water for hydrogeochemical analyses including isotopes was taken into the sample bottles immediately from the end of the pumping tube and the sample pretreatment, filtering and acidification, was performed in the

field after sampling. Water samples for oxygen and hydrogen isotope analyses were collected without pretreatment and stored in 60 mL high-density polyethylene (HDPE) bottles. For isotopic analyses of strontium and sulphur groundwater was filtered with a 0.45 µm Ca–S filter into acid-washed 250 mL bottles and acidified with ultrapure 13.8 N HNO<sub>3</sub> (5 mL per sample bottle). Treated samples were kept cool during field work and transportation to the laboratory. The chemical parameters from the water samples were analysed by the Eurofins Labtium laboratory (Espoo, Finland). Dissolved element concentrations were analysed with ICP-MS and anion concentrations (Br<sup>-</sup>, Cl<sup>-</sup>, F, NO<sub>3</sub><sup>-</sup> ja SO<sub>4</sub><sup>2-</sup>) with ion chromatography. The dissolved and total organic carbon (DOC, TOC) were also analysed at the Eurofins Labtium.

### 2.2 Isotope hydrogeochemistry analyses

The isotopic compositions of oxygen, hydrogen, strontium and sulphur from the water samples were analysed in the GTK research laboratory in Espoo, Finland. Sample waters for the δ<sup>18</sup>O and δ<sup>2</sup>H analyses were filtered in the laboratory and analysed with a Picarro L2130i CRDS (Cavity Ring Down Spectroscopy) analyser. The measurement uncertainty for δ<sup>18</sup>O being < 0.1 ‰, and for δ<sup>2</sup>H < 0.3 ‰. For the <sup>87</sup>Sr/<sup>86</sup>Sr analysis, a concentration-dependent amount of prefiltered and -acidified samples were evaporated to dryness and dissolved with ultrapure 3.2 N HNO<sub>3</sub> for ion exchange. Strontium was eluted with ultrapure 0.05 N HNO<sub>3</sub> acid by 100 µL of Sr-specific resin (TrisKem Sr Resin, 50–100 µm). For the measurement, the samples were diluted to a Sr concentration of approx. 20 ppb (in ultrapure 2 % HNO<sub>3</sub>). The analyses were carried out by using an Aridus 3 Desolvating system (DSN) with 50 µL PFA ConcentricFlow nebulizer and a Multi-Collector Inductively Coupled Plasma Mass Spectrometer (MC-ICP-MS, Nu Instruments™) at low mass resolution ( $\Delta m/m = 400$ ). The isotopic measurements were performed in static mode using five faraday detectors, and 10 blocks of 6 integrations of approximately 8 s. The standard reference material NBS987, was used to monitor the precision and accuracy of the measurements at the beginning, and the end of every session and after every fifth sample. The obtained average of <sup>87</sup>Sr/<sup>86</sup>Sr was 0.710270 (±0.000066, 2 SD, *n* = 5), which is close to the reference value 0.710250 (±0.00004, 2 SD, *n* = 2306, GEO-REM database, <http://georem.mpch-mainz.gwdg.de/>, last access: 30 April 2025).

Prior to the δ<sup>34</sup>S analysis, samples were eluted following the classic liquid column chromatography technique (Paris et al., 2013). Based on the sulphur concentration, part of the filtered and acidified sample was evaporated to dryness and dissolved with ultrapure 0.25 % HCl. Cations were removed with BioRad AG50X8 resin and samples were further diluted with ultrapure 2 % HNO<sub>3</sub> to approx. 0.25 ppm concentration. Sodium was added to the samples (0.5 ppm) before the analysis to improve the sensitivity of sulphur (Yu et al., 2017).

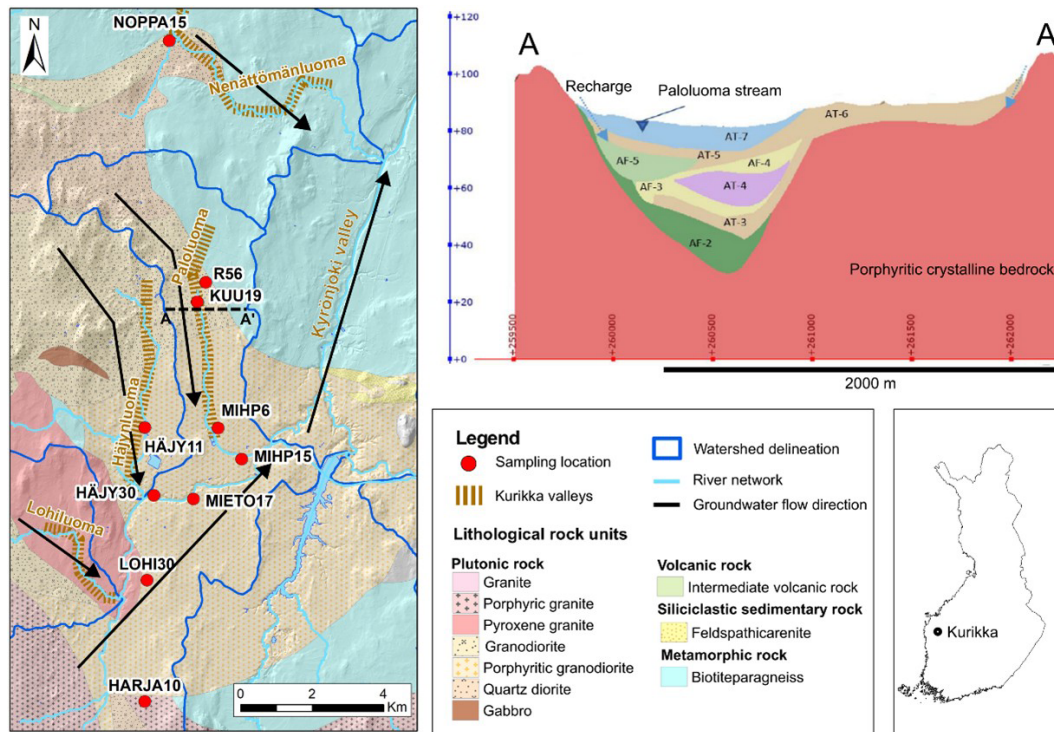


**Figure 1.** Left, a geological map of the study area and groundwater sampling locations; right: general cross-section of the Paloluoma buried valley (modified from Rashid, 2022). Arrows in the map indicate potential groundwater flow paths. AF- and AT- refer to aquifer and aquitard, respectively in the cross-section. AT 3-4-5-6: till, AF3-4: fine sand, AF2: sandy gravel, AF5: coarse sand. See also Table 1. Vertical exaggeration: 15×.

**Table 1.** Details of the sampling sites in Kurikka multilayer aquifer system.

Sample ID	Sampling date	Location	Total depth of the well, m	Screen depth interval, m	Aquifer code <sup>a</sup> /type
NOPPA 15	4 October 2021	Nenättömänluoma	15.6	6.6–9.1; 10.6–13.6 <sup>b</sup>	AF7A; Shallow unconsolidated
MIHP6	5 October 2021	Paloluoma	77.7	50.9–76.9	AF3A; Deep unconsolidated
MIHP15	5 October 2021	Paloluoma	64.6	38.1–64.6	AF3A; Deep unconsolidated
R56	5 October 2021	Paloluoma	162 <sup>c</sup>	no screen <sup>c</sup>	Not available; Bedrock
LOHI30	5 October 2021	Lohiluoma	78.4	50.4–64.4	AF3A; Deep unconsolidated
KUU19	6 October 2021	Paloluoma	72.9	49.5–72.9	AF3A; Deep unconsolidated
HÄJY30	6 October 2021	Kyrönjoki main valley	17.4	no screen <sup>d</sup>	AF3A; Deep unconsolidated
MIETO17	6 October 2021	Kyrönjoki main valley	63.8	29.8–48.8; 49.8–60.8 <sup>b</sup>	AF3A; Deep unconsolidated
HARJA10	7 October 2021	Kyrönjoki main valley	60.8	37.8–39.8; 41.8–51.8 <sup>b</sup>	AF3A; Deep unconsolidated
HÄJY11	7 October 2021	Häjinluoma	59	39–59	AF4B; Deep unconsolidated

<sup>a</sup> Described in more details in Åberg et al. (2026).

<sup>b</sup> Two screens.

<sup>c</sup> Bedrock borehole, no screen in the sediment layers. Total length of borehole in the table. Drilled with 60° dip.

<sup>d</sup> No screen. Observation well has a total depth of 17.4 m and is open at its base. Continuously overflowing.

The analyses were carried out using an Aridus 3 Desolvating system (DSN) with 50 µL PFA ConcentricFlow nebulizer and a MC-ICP-MS (Nu Instruments™) at medium mass resolution ( $\Delta m/m = 3000$ ). The S isotopic measurements were performed in static mode using three faraday detectors, and 3 blocks of 20 integrations of 8 s. The average value of the

IAEA standard S-3 was  $-32.0 (\pm 0.3, 1 \text{ SD}, n = 5)$  while the recommended values is  $-32.2 (\pm 0.4\%, 1 \text{ SD}, n = 36)$ , Georem database, <http://georem.mpch-mainz.gwdg.de/>, last access: 30 April 2025).

### 2.3 Residence time indicator sampling and analysis

Atmospheric CFC concentrations increased since the late 1940 to early 1990 and are nearly stable in the atmosphere. During recharge these tracers are dissolved in the water and transported with the flow. The CFC concentrations in water depend not only on the time of recharge, but also on the recharge temperature of the water, additional dissolved air bubbles (so-called excess air) and degradation in anoxic environment. SF<sub>6</sub> has been released decades later. Atmospheric concentrations are still increasing but are still much lower than for CFCs. Due to the very low solubility excess air affects the signal even more. Also, in granitic rocks, SF<sub>6</sub> is produced by natural processes over long timescales.

The radioactive hydrogen isotope tritium (<sup>3</sup>H) with a half-life of 12.32 years is bound to the water molecule in precipitation.

Tritium concentrations in precipitation increased since the mid-1950s to about 1962 by 3 orders of magnitude compared to the natural concentrations in the northern hemisphere. Since 2010 concentrations are nearly back to natural levels (Cauquoin et al., 2024). Tritium is a suitable tracer to detect water recharged since the late 1950s, which is called young water.

In combination with the decay product of <sup>3</sup>H, the light helium isotope <sup>3</sup>He, it is possible to calculate the groundwater residence time without knowledge of the initial <sup>3</sup>H input. The challenge is to separate <sup>3</sup>He from <sup>3</sup>H decay (tritogenic <sup>3</sup>He) from other He sources. Atmospheric <sup>3</sup>He is dissolved in surface water according to the water temperature at recharge. The water can contain additional air bubbles (excess air) and depending on the rock matrix also terrigenous <sup>3</sup>He. This is produced by neutrons reacting with <sup>6</sup>Li which produces <sup>3</sup>H, and hence <sup>3</sup>He. The neutrons originate from U and Th decay and associated secondary reactions, and are accompanied by <sup>4</sup>He produced through the alpha decay of U and Th. Consequently, both <sup>4</sup>He and <sup>3</sup>He concentrations can be elevated in old groundwater. The concentrations and <sup>3</sup>He/<sup>4</sup>He ratio depend on the rock matrix composition, and the release rate from the rock to the surrounding water body. This results in significant uncertainties in the <sup>3</sup>He/<sup>4</sup>He ratio of terrigenous He. Consequently, at high helium concentrations, the separation of tritogenic <sup>3</sup>He is hindered. Tritogenic <sup>3</sup>He (<sup>3</sup>He<sub>tri</sub>) is calculated as follows from the components:  ${}^3\text{He}_{\text{tri}} = {}^3\text{He}_{\text{meas}} - {}^3\text{He}_{\text{equi}} - {}^3\text{He}_{\text{excess}} - {}^3\text{He}_{\text{terr}}$ ; <sup>3</sup>He<sub>meas</sub>: measured concentration, <sup>3</sup>He<sub>equi</sub>: solubility equilibrium concentration, <sup>3</sup>He<sub>excess</sub>: excess air concentration derived from Ne, <sup>3</sup>He<sub>terr</sub>: terrigenous He concentration derived from <sup>4</sup>He. The uncertainties for each component add up to uncertainty for <sup>3</sup>He<sub>tri</sub>. A detailed explanation on the different <sup>3</sup>He contributions can be found in Kipfer et al. (2002). Samples of groundwater for CFCs and SF<sub>6</sub> analyses were collected in two tins, each holding a ground glass flask. The opened can and flask were placed in a bucket. Then, the pipe from the pump was placed to the bottom of the flask,

which was rinsed multiple times until the bucket overflowed. After the flask was closed with a plug and secured with a clamp, the can container was closed with a circlip (underwater). CFCs and SF<sub>6</sub> were analysed by gas chromatography with an electron capture detector (GC-ECD) at Dr. Oster's trace substances laboratory (Wachenheim, Germany). Samples for <sup>3</sup>H analysis were collected in 1 L HDPE bottle and stored in a cold room (5 °C) until analysis. Tritium was analysed at Hydroisotop GmbH (Germany) using liquid scintillation spectroscopy LSC after electrolytical enrichment (Perkin Elmer Quantulus GCT 6220). Tritium concentrations are reported in <sup>3</sup>H units (TU) with double standard deviation (1 TU = 0.119 Bq L<sup>-1</sup>). Samples for noble gases analyses were collected in duplicates in clamped-off copper tubes connected to the pumping line. Noble gases (helium isotopes and neon) were analysed at the Bremen Mass Spectrometric Facility according to Sültenfuß et al. (2009).

### 2.4 Microbiological sampling and analysis

Groundwater samples were retrieved for microbial community structure analysis. As groundwater is a naturally oligotrophic environment, the microbial cell numbers were estimated to be low. Therefore, to collect enough microbial biomass for DNA amplicon sequencing analysis, 65–183 L of groundwater from each groundwater well was filtered by a dead-end ultrafiltration method (DEUF) with a flow rate of 2–3 L min<sup>-1</sup> using a sterile silicone tubing with an ultrafiltering cartridge (ASAHI Rexeed-25A, Asahi Kasei Medical Co., Ltd., Tokyo, Japan), according to Inkinen et al. (2019). Groundwater was pumped from the wells to a 20 L plastic canister sterilized with 70 % EtOH and flushed with the sampling fluid, from where the water was pumped through the DEUF capsule cartridge with a peristaltic pump. The flow-through was measured using a water meter and a 10 L bucket. DEUF-capsules were kept cool during field work and transportation to further handling the laboratory of water microbiology of the Finnish Institute for Health and Welfare, Kuopio.

Microbial biomass was eluted from the DEUF-capsules in laboratory as described in Inkinen et al. (2019). The secondary concentration of DEUF-eluates (100–250 mL, corresponding to sample volume of 11–80 L) was conducted by filtration through Millipore Express PLUS membrane filters (pore size 0.22 μm, Merck KGaA, Darmstadt, Germany (Kauppinen et al., 2019) and stored in –75 °C before nucleic acid extraction. Total nucleic acids were extracted from the Express PLUS filters using Chemagic DNA Plant kit (Perkin-Elmer, Waltham, USA) and Kingfisher device (Thermo Fisher Scientific, Waltham, MA, USA) and DNA concentration was measured with a Qubit mini fluorometer using Qubit dsDNA HS assay (Thermo Fisher Scientific, Waltham, MA, USA) as described in Inkinen et al. (2019). Negative control samples of DEUF elution and DNA extraction were also included in the analysis. MiSeq

amplicon sequencing of the 16S rRNA gene of bacteria and archaea, and ITS1 region for fungi using  $2 \times 300$  bp paired end protocol was done in commercial laboratory (Eurofins Genomics Ltd., Konstanz, Germany). The primers used were 341F 5'-CCTACGGGNGGCWGCAG-3' (Herlemann et al., 2011) and 926R 5'-CCGYCAATYMTTTRAGTTT-3' (Quince et al., 2011) (V3–V5) for bacteria, 340F 5'-CCCTAYGGGGYGCASCAG-3' (Gantner et al., 2011) and 806R 5'-GGACTACNVGGGTWTCTAAT-3' (Apprill et al., 2015) (V3–V4) for archaea, and 5'-GGAAGTAAAAGTCGTAACAAGG-3' and 5'-GCTGCGTTCTTCATCGATGC-3' for fungal ITS1 (White et al., 1990). Negative controls did not produce amplicons.

Sequence reads were demultiplexed and primer sequences removed before analysis applying the DADA2 (v.1.30.0) pipeline in Rstudio using R version 4.3.2 (Callahan et al., 2016; R Core Team, 2024) for bacterial and archaeal amplicon sequence variant (ASV) detection. When inspecting the sequence reads, reverse reads of both archaea and bacteria were of poor quality, generating issues in trimming and eventually merging the reads. Thus, the analysis was continued with just forward reads. Reads were filtered using the following parameters (TruncLen = 240, maxN = 0, maxEE = 2, truncQ = 2). This removed approximately 4 % of reads in each sample. Reads were dereplicated, sequence variants inferred from unique sequences from each sample, chimeras removed, and taxonomy assigned using Silva v. 138 taxonomy database (silva\_nr99\_v138.1\_train\_set.fa) (Quast et al., 2013; Yilmaz et al., 2014) for archaea and bacteria.

Fungal sequences were analysed using the ITS-specific variation of version 1.8 of the DADA2 workflow (Callahan et al., 2016). First, ITS primer sequences were detected, primer orientation was verified, and primers were cut from the sequences using Cutadapt tool (Martin, 2011). After quality trimming with parameters: maxN = 0, maxEE =  $c(2, 2)$ , truncQ = 2, minLen = 50, rm.phix = TRUE, sequence variants were inferred from unique sequences from each sample, forward and reverse reads were merged, chimeras removed and taxonomy assigned using UNITE general FASTA release (sh\_general\_release\_dynamic\_04.04.2024.fasta) (Abarenkov et al., 2024) for fungi.

DADA2-treated sequence data were imported to phyloseq (v.1.46.0) (McMurdie and Holmes, 2013) for data visualisation and statistical analyses in RStudio. Tools used in RStudio included vegan, ggplot2, dplyr, ampvis2, psadd and cowplot (Andersen et al., 2018; Oksanen et al., 2025; Wickham, 2016; Wickham et al., 2026; Wilke, 2025). Raw sequence data is deposited in NCBI's SRA under BioProject PRJNA1270735.

### 3 Results

#### 3.1 Field observations and hydrogeochemistry

Field parameters and the calculated partial pressure of CO<sub>2</sub> ( $p\text{CO}_2$ ) are presented in Table 2. The unconsolidated aquifer groundwaters had an electrical conductivity ranging from 90–204  $\mu\text{S cm}^{-1}$  and a pH between 6.2 and 6.8, whereas the water from the bedrock borehole was more mineralized (EC 296  $\mu\text{S cm}^{-1}$ ) and had a higher pH (8.4). Temperature range was 5.7–6.9 °C, and highest dissolved oxygen concentrations were measured at KUU19 and HÄJY30 (5.7 and 4.4  $\text{mg L}^{-1}$ , respectively). The field data clustered the samples to three groups, R56 clustering clearly separate from the other sites. Oxidation-reduction potential varied significantly between the different samples from lowest in bedrock groundwater R56 (−254 mV) to highest in HÄJY11 and KUU19, corresponding to high dissolved oxygen concentrations in these samples. Highest Cl<sup>−</sup> concentration was measured from the bedrock groundwater (R56). Alkalinity varied from 23.5  $\text{mg L}^{-1}$  in KUU19 to 152  $\text{mg L}^{-1}$  in R56. In all groundwater samples representative of unconsolidated aquifer waters, log partial pressure of CO<sub>2</sub> ( $p\text{CO}_2$ ) values ranged between −1.4 and −2.2 atm while the lowest log  $p\text{CO}_2$  value in the dataset (−3.3) was observed in bedrock groundwater.

The major ions in groundwaters were Na (46.5  $\text{mg L}^{-1}$  in R56 to 4.82  $\text{mg L}^{-1}$  in HARJA10), Cl (25  $\text{mg L}^{-1}$  in R56 to 1.7  $\text{mg L}^{-1}$  in MIHP6, see Table S1 for laboratory measurements), and Fe (31.5  $\text{mg L}^{-1}$  in HARJA10, below the detection limit of 0.03  $\text{mg L}^{-1}$  in HÄJY11 and KUU19 and 0.08  $\text{mg L}^{-1}$  in MIHP6), and Ca, with highest concentrations in NOPPA15 and HÄJY30 (14.8 and 15.8  $\text{mg L}^{-1}$ , respectively) (Table S1). Highest sulphur and sulphate concentrations were detected from NOPPA15, and highest organic carbon concentrations were in HARJA10 groundwater (Table S1).

Groundwater types were defined and represented on a Piper diagram (Fig. 2) showing the proportion of major ions (Na<sup>+</sup>, Ca<sup>2+</sup>, Mg<sup>2+</sup>, K<sup>+</sup>, HCO<sub>3</sub><sup>−</sup>, Cl<sup>−</sup>, SO<sub>4</sub><sup>2−</sup>) (Piper, 1944, Simler 2012). Unconsolidated aquifer groundwater samples are of calcium-bicarbonate (Ca–HCO<sub>3</sub>) type or mixed cations–HCO<sub>3</sub>, whereas groundwater collected from the bedrock borehole (R56) beneath the Paloluoma valley is classified as sodium-bicarbonate (Na–HCO<sub>3</sub>) type, reflecting a more evolved groundwater. NOPPA15 has more chloride (7.6  $\text{mg L}^{-1}$ ) than the other unconsolidated aquifer samples (1.7–5.1  $\text{mg L}^{-1}$ ) and KUU19 has some nitrates (4.6  $\text{mg L}^{-1}$ ) (Table S1).

#### 3.2 Isotopic compositions of hydrogen and oxygen

The variation in the isotopic compositions of oxygen and hydrogen in the analysed water samples was small. The  $\delta^2\text{H}$  values range from −91 ‰ to −88.2 ‰ and the  $\delta^{18}\text{O}$  from

**Table 2.** Field measurement data of pH, electrical conductivity (EC), temperature ( $T$ ), dissolved oxygen (DO), oxygen reduction potential (ORP), alkalinity (Alk), chloride concentration ( $\text{Cl}^-$ ) from the sampling sites and calculated  $p\text{CO}_2$ . Clustering is based on the field measurements (in bold) and shows the average Euclidean dissimilarity between the samples.

Sample ID	pH	EC $\mu\text{S}/\text{cm}$	T $^{\circ}\text{C}$	DO $\text{mg}/\text{l}$	ORP $\text{mV}$	$\text{Cl}^-$ $\text{mg}/\text{l}$	Alk. (as	log $p\text{CO}_2$
							$\text{HCO}_3^-$ ) $\text{mg}/\text{l}$	
MIETO17	6,3	124,4	6,4	3,5	17,9	2,9	<b>68,3</b>	-1,6
MIHP6	6,8	118,0	5,9	3,3	50,5	2,2	<b>48,8</b>	-2,2
HÄJY30	6,7	204,5	6,3	4,4	-52,3	6,6	<b>115,9</b>	-1,7
KUU19	6,4	89,9	6,2	5,7	104,4	4,1	<b>23,5</b>	-2,2
LOHI30	6,6	165,2	6,4	2,7	96,0	4,6	<b>112,2</b>	-1,6
HARJA10	6,5	178,8	5,7	3,4	-91,6	7,1	<b>92,7</b>	-1,7
MIHP15	6,6	162,7	6,8	3,9	-50,9	n.a.*	<b>83,0</b>	-1,8
HÄJY11	6,7	97,2	6,2	3,1	109,2	1,3	<b>37,8</b>	-2,2
NOPPA15	6,2	188,8	6,1	2,7	-0,2	10,8	<b>78,1</b>	-1,4
R56	8,4	296,2	6,9	2,7	-254,0	26,6	<b>152,5</b>	-3,3

\* n.a.: Not available, laboratory measurements of chloride concentrations are reported in Table S1 in the Supplement.

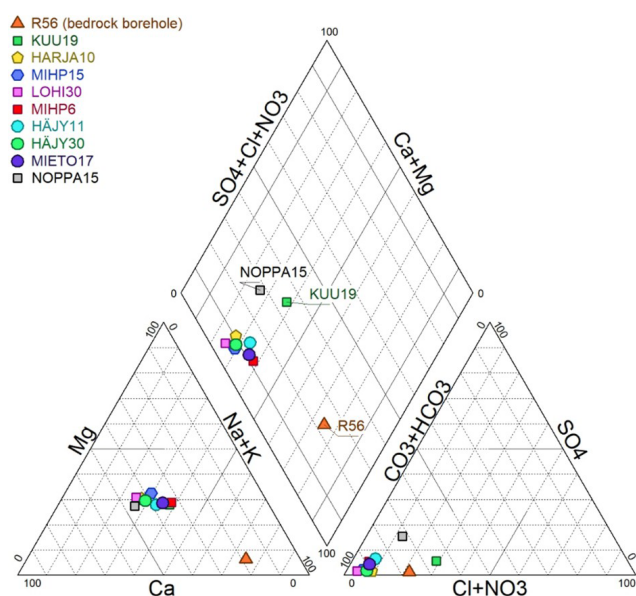


**Figure 2.** Piper diagram for the 10 groundwater samples collected in the study area.

–12.63‰ to –12.22‰ (with the analytical uncertainty for  $\delta^{18}\text{O}$  is  $< 0.1\%$  and for  $\delta^2\text{H} < 0.3\%$ ). In the Fig. 3 the weighted annual average from the south-western coastal site of Olkiluoto and the eastern Finnish city of Kuopio (GNIP database, IAEA), with similar latitude to the study site, are marked on the meteoric water line. The  $d$ -excess values Eq. (1), calculated from  $\delta^2\text{H}$  and  $\delta^{18}\text{O}$  values, ranged from 9.6–10.8, indicating that the sampled waters are unevaporated and of meteoric origin. This is reinforced by the fact that the samples all plot on or near the meteoric water lines (Table 3 and Fig. 3).

$$d\text{-excess} = \delta^2\text{H} - 8 \times \delta^{18}\text{O} \quad (1)$$

### 3.3 Isotopic compositions of Sr and S

The isotopic compositions of strontium and sulphur in the water samples vary between 0.72133–0.75237 and 1.1‰–30.3‰ respectively (Table 3). The corresponding concentrations of Sr and S in the water samples vary between 38.3–107  $\mu\text{g L}^{-1}$  and 0.1–5.9  $\text{mg L}^{-1}$  respectively (Tables 3 and S1). Both elements show noticeable variation (Table 3).

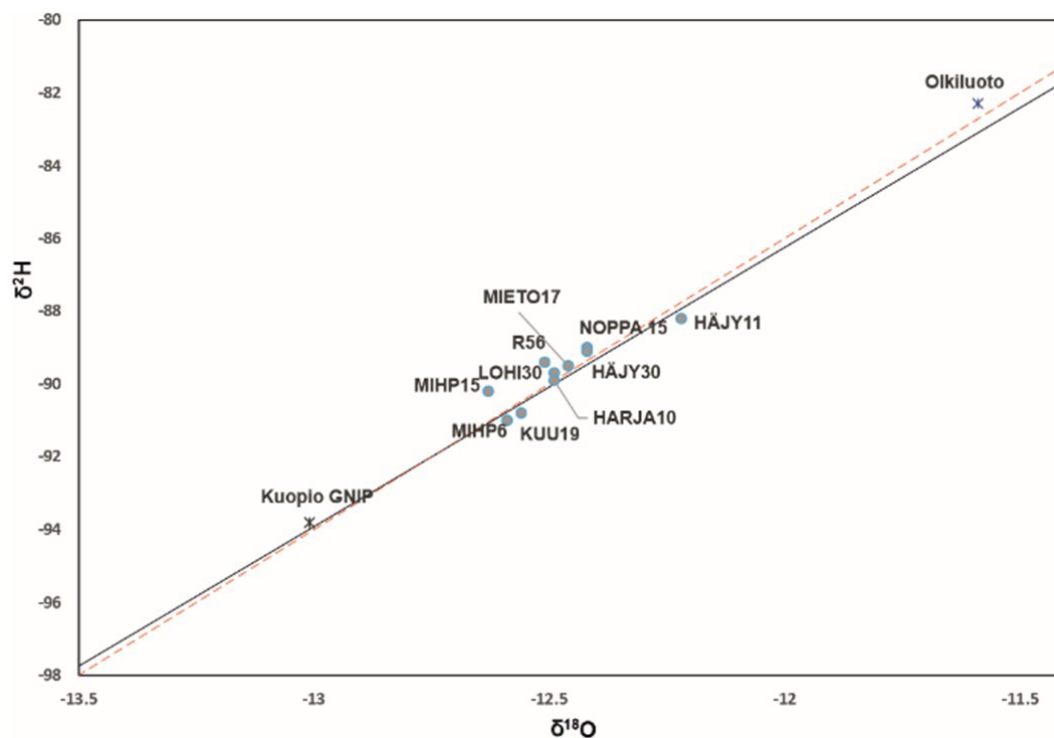
### 3.4 Groundwater residence time indicators

The results of the  $^3\text{H}$ ,  $^3\text{He}$ , neon,  $\text{SF}_6$  and CFCs analyses are listed in Table 4. Samples NOPPA15, KUU19, HARJA10 and HÄJY11 had  $^3\text{H}$  concentrations ranging from 1.6–4.8 TU, while samples MIHP6, MIETO17, MIHP15, R56, LOHI30 and HÄJY30, were below the detection limit of 0.6 TU (2-sigma) (Table 4). Tritium concentrations between 1.6 and 4.8 TU (NOPPA15, KUU19, HARJA10, HÄJY11) clearly show a modern component (0–60 years old). Assuming a decay-corrected  $^3\text{H}$  concentration in precipitation to be near natural levels of 4–5 TU for Finland, then the HÄJY11 shows the presence of a modern component with significant dilution of 2/3 older  $^3\text{H}$ -free water. The absence of  $^3\text{H}$  ( $< 0.6\text{ TU}$ ) indicates sub-modern waters with ages exceeding 70 years. Due to the given detection limit this proportion of modern water cannot be significantly larger than 15%. Hence, only the samples with  $^3\text{H}$  the calculation of  $^3\text{H}$ – $^3\text{He}$  ages is possible.

The applicability of CFCs and  $\text{SF}_6$  for groundwater residence time determination is very limited for this study. The CFCs data exhibit anomalous concentrations and variable CFC11 / CFC12 ratios, indicating contamination or degradation processes. The data show that  $^3\text{H}$ -free waters do not contain any CFC11 or CFC12. This means that the sampling gear is not responsible for the extreme high CFC concentra-

**Table 3.** The isotopic analysis results and the calculated *d*-excess values together with the concentrations of strontium and sulphur in the water samples.

ID	$\delta^2\text{H}$ (‰)	$\delta^{18}\text{O}$ (‰)	<i>d</i> -excess	$^{87}\text{SR}/^{86}\text{SR}$	SR ( $\mu\text{g L}^{-1}$ )	$\delta^{34}\text{S}$ (‰)	S ( $\text{mg L}^{-1}$ )
NOPPA 15	−89.0	−12.42	10.4	0.74535	101	1.1	5.87
MIHP6	−91.0	−12.59	9.7	0.74029	46.7	8.0	0.7
MIHP15	−90.2	−12.63	10.8	0.72133	82.7	12.6	0.34
R56	−89.4	−12.51	10.7	0.73225	91.6	23.8	0.5
LOHI30	−89.7	−12.49	10.2	0.74159	86	30.3	0.26
KUU19	−90.8	−12.56	9.7	0.75237	38.3	5.9	0.39
HÄJY30	−89.1	−12.42	10.3	0.72832	107	14.1	0.57
MIETO17	−89.5	−12.46	10.2	0.73679	70.8	5.3	0.93
HARJA10	−89.9	−12.49	10.0	0.73713	74	18.5	< 0.2
HÄJY11	−88.2	−12.22	9.6	0.73752	56.5	8.8	0.64

**Figure 3.** The isotopic compositions of oxygen and hydrogen from the water samples against the GMWL (Global Meteoric Water line) in red dashed line and the LMWL (Local Meteoric Water Line) in black. Olkiluoto weighted 8 year annual mean ([https://inis.iaea.org/collection/NCLCollectionStore/\\_Public/46/095/46095041.pdf](https://inis.iaea.org/collection/NCLCollectionStore/_Public/46/095/46095041.pdf), last access: 7 May 2025) and Kuopio GNIP, Global Network of Isotopes in Precipitation (<https://www.iaea.org/services/networks/gnip>, last access: 7 May 2025) as references.

tions. Concentrations of CFC113 in all samples were at or below the detection limit and were therefore excluded from further analysis.

All samples showed  $\text{SF}_6$  contents ( $18\text{--}2700\text{ fmol L}^{-1}$ ) well above solubility equilibrium with modern atmosphere (approx.  $4\text{ fmol L}^{-1}$ ), indicating that the excessive groundwater concentrations derive from a local geogenic source, as frequently observed in Scandinavian groundwater systems (Åkesson et al., 2015). Consequently, CFCs and  $\text{SF}_6$  tracers are unsuitable for groundwater age dating at this site. The

data are nevertheless shown to illustrate the limitations of these methods under the studied conditions.

Seven out of ten noble gas samples have been analysed in duplicates and provided identical results. Neon concentrations reveal abnormal excess air (more than  $2 \times 10^{-7}\text{ ccSTP g}^{-1}$ ), which diminishes reliable age calculations based on noble gases. For the analysis of samples with high  $^4\text{He}$  concentrations, the amount of gases was split to small units. This increased the uncertainty for Ne to about 1 % of the He concentration.

**Table 4.** Summary of measured  $^3\text{H}$  concentrations, calculated tritiogenic Helium 3 ( $^3\text{He}_{\text{trit}}$ ),  $^3\text{He}/^4\text{He}$  ratio, calculated terrigenic Helium 4 ( $^4\text{He}_{\text{terr}}$ ), CFC and  $\text{SF}_6$  concentrations. The uncertainty of  $\text{SF}_6$  is 20 %. Tritiogenic Helium 3 was determined with an altitude of the recharge area of 150 m and a recharge temperature of 5 °C.

Sample	$^3\text{H}$ TU	$^3\text{He}_{\text{trit}}$ TU	$^3\text{He}/^4\text{He}$	$^4\text{He}$ ccSTP g $^{-1}$	$^4\text{He}_{\text{terr}}$ ccSTP g $^{-1}$	Ne ccSTP g $^{-1}$	Ne/He	$\text{SF}_6$ fmol L $^{-1}$	CFC11 pmol L $^{-1}$	CFC12 pmol L $^{-1}$
NOPPA15	4.8 ± 0.6	88	3.62 × 10 $^{-7}$	1.03 × 10 $^{-6}$	9.31 × 10 $^{-7}$	3.90 × 10 $^{-7}$	0.38	18	13 ± 3	1.4 ± 0.1
MIHP6	< 0.6	–	1.61 × 10 $^{-7}$	1.89 × 10 $^{-6}$	1.65 × 10 $^{-6}$	8.76 × 10 $^{-7}$	0.46	2700	< 0.05	< 0.05
MIHP15	< 0.6	–	4.08 × 10 $^{-8}$	7.25 × 10 $^{-6}$	7.12 × 10 $^{-6}$	5.06 × 10 $^{-7}$	0.07	75	< 0.05	< 0.05
R56	< 0.6	–	2.8 × 10 $^{-8}$	1.02 × 10 $^{-4}$	1.02 × 10 $^{-4}$	8.56 × 10 $^{-7}$	0.01	27	< 0.05	< 0.05
LOHI30	< 0.6	–	1.30 × 10 $^{-7}$	1.86 × 10 $^{-6}$	1.68 × 10 $^{-6}$	6.62 × 10 $^{-7}$	0.36	990	0.08 ± 0.05	< 0.05
KUU19	3.8 ± 0.7	107	9.40 × 10 $^{-7}$	4.55 × 10 $^{-7}$	3.42 × 10 $^{-7}$	4.38 × 10 $^{-7}$	0.96	110	230 ± 10	2.1 ± 0.2
HÄJY30	< 0.6	–	6.6 × 10 $^{-8}$	3.70 × 10 $^{-6}$	3.52 × 10 $^{-6}$	6.88 × 10 $^{-7}$	0.19	2200	0.5 ± 0.1	< 0.05
MIETO17	< 0.6	–	7.1 × 10 $^{-8}$	3.51 × 10 $^{-6}$	3.34 × 10 $^{-6}$	6.28 × 10 $^{-7}$	0.18	100	0.19 ± 0.05	< 0.05
HARJA10	4.6 ± 0.6	61	1.36 × 10 $^{-6}$	1.71 × 10 $^{-7}$	1.13 × 10 $^{-7}$	2.49 × 10 $^{-7}$	1.46	140	0.07 ± 0.05	< 0.05
HÄJY11	1.6 ± 0.7	41	2.09 × 10 $^{-7}$	1.98 × 10 $^{-6}$	1.78 × 10 $^{-6}$	7.42 × 10 $^{-7}$	0.38	32	0.17 ± 0.05	0.09 ± 0.05

Samples with large excess air and non-detectable CFC concentration clearly state that the source of excess air does not result from ambient air, such as air penetration into the water during sampling. As typical groundwater recharge conditions are not expected to form this massive intrusion of excess air, the source remains unclear.

Nevertheless, He isotopes still give some insight on the age composition of the water. All samples show high  $^4\text{He}$  concentrations, ranging from  $4.55 \times 10^{-7} - 1.0 \times 10^{-4}$  ccSTP g $^{-1}$ , which is equivalent to 4–2200 times the solubility equilibrium, indicating a significant source of terrigenic He. The  $^3\text{He}/^4\text{He}$  ratios in  $^3\text{H}$ -free samples range from  $3 \times 10^{-8} - 7 \times 10^{-8}$ , which are significantly lower than the ratios typical of atmospheric or mantle He. The  $^3\text{He}/^4\text{He}$  ratio of  $2 \times 10^{-8}$  is used for the terrigenic He component in the calculation of tritiogenic  $^3\text{He}$  for samples with  $^3\text{H}$ . Excess air is assumed to be free of tritiogenic  $^3\text{He}$  (Fig. 4). Both error sources result in an error for tritiogenic  $^3\text{He}$  of 25 %. However, even with the large uncertainties the  $^3\text{H}$ – $^3\text{He}$  ages of NOPPA15, KUU19, HARJA10 and HÄJY11 are between 47 and 59 years ( $\pm 25\%$ ). These results suggest groundwater residence times substantially longer than 30 years. The presence of high radiogenic Helium 4 ( $^4\text{He}_{\text{rad}}$ ) indicates the presence of old groundwater (several thousand years old). The only bedrock borehole R56 has the highest radiogenic helium contents of all the wells.

### 3.5 Microbial communities

Bacterial 16S rRNA amplicon sequencing was successful from HARJA10, HÄJY30, LOHI30, MIETO17, MIHP15, NOPPA15 and R56. Altogether 996 645 bacterial sequences were retrieved of these, and after quality filtering, denoising and chimera removal steps, 90%–94% of the reads were retained in each sample (Table S2). Altogether 71 different bacterial phyla were detected and ASVs belonging most prevalently to Patescibacteria, Verrucomicrobiota, Chloroflexi and Proteobacteria (Table S3 and Fig. S1a in the Supplement).

Bacterial communities were diverse and varied from borehole to borehole (Figs. 5A and S1a). NOPPA15 hosted the most diverse bacterial community according to Shannon index ( $H'$  6.69), while MIHP15 and bedrock groundwater well R56 exhibited the lowest observed Shannon diversity ( $H'$  3.63 and 2.91, respectively) (Fig. 5A and Table S2.). These communities were more similar with each other compared to other sites. Relatively most abundant bacterial ASVs detected from NOPPA15 affiliated with *Gallionella* (12% relative abundance), *Omnitropha* (10%) and several candidate genera of Patescibacteria phyla. The bedrock borehole water R56 hosted a bacterial community with abundant sulfate reducers such as *Desulfovibrio* (38% relative abundance) in addition to *Hydrogenophaga* (11%), *Ferribacterium* (9%) and *Acetobacterium* (8%). Of these, *Hydrogenophaga*-affiliating ASVs were either absent or found in very low abundance (< 0.2%) in other samples. *Desulfovibrio* and *Acetobacterium* ASVs were also most abundant in MIHP15 (57% and 11%, respectively). Sulfate reducing *Desulfosporosinus* was also most abundant in HÄJY30 (65% of the bacterial community), together with *Candidatus Omnitrophus* (12% relative abundance) and Patescibacteria-affiliating ASVs (altogether 7% of total bacterial community). MIETO17 hosted almost as diverse bacterial community as NOPPA15 according to Shannon diversity index ( $H'$  6.52). Abundant ASVs in MIETO17 affiliated with *Desulfovibrio* (10%), *Dehalococcoidia* (9%), *Rhodospirillum rubrum* (6%), *Omnitrophus* and Patescibacteria (6% relative abundance each), Nitrospirota (4%) and Sva0485, recently named as *Candidatus Acidulodesulfobacterales* (Tan et al., 2019) (3%). Most common ASVs in LOHI30 were *Candidatus Omnitrophus* (13%), *Ferribacterium* (8%), *Acetobacterium* (8%), *Dehalococcoidia* (7%), *Rhodospirillum rubrum* (6%), *Desulfurivibrio* (6%), and *Gallionella* (4%). Similarly, in HARJA10, *Candidatus Omnitrophus* was among the most dominant ASVs (13% relative abundance) together with *Desulfovibrio* (16%), Sva0485 (10%) and *Dehalococcoidia* (8%).

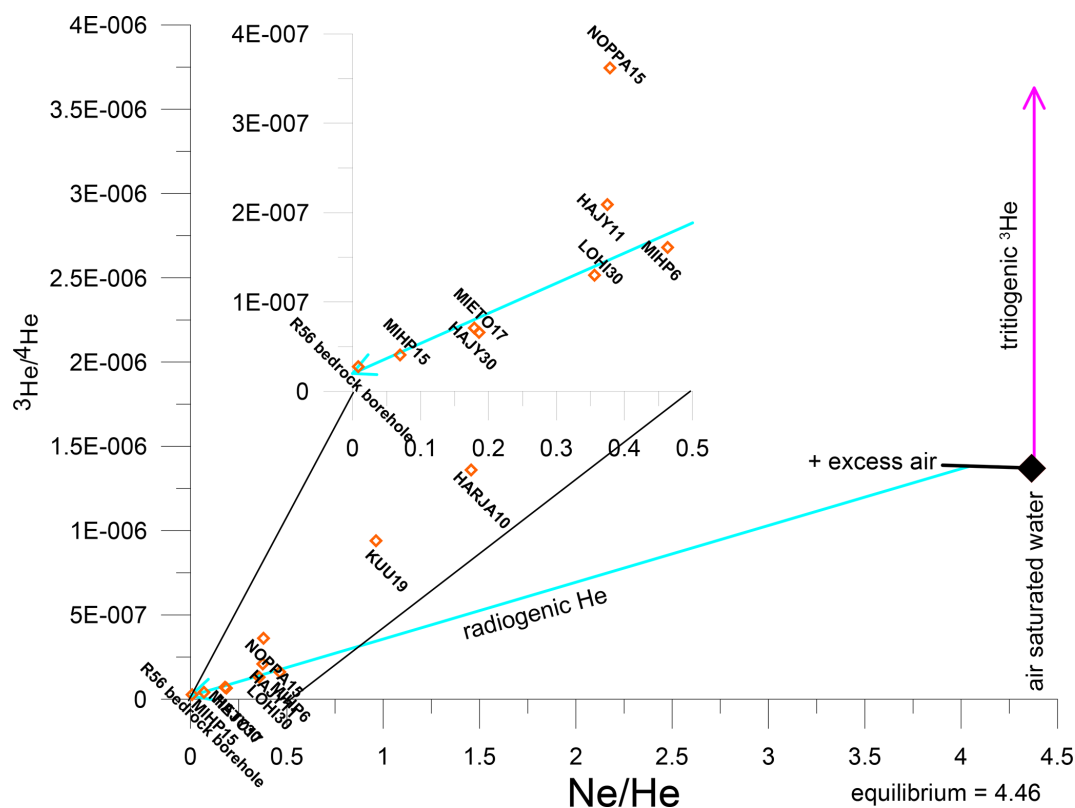


**Figure 4.** Ratios of He isotopes vs. Ne/He ratios of all samples. The light blue line shows mixing of water equilibrated at 5 °C plus 30 % of excess air with terrigenous He that has a  $^3\text{He}/^4\text{He}$  of  $2 \times 10^{-8}$ . The vertical offset from this line indicates tritiogenic  $^3\text{He}$ .

Archaeal 16S rRNA amplicon sequencing was successful from HARJA10, HÄJY30, MIETO17, MIHP15, NOPPA15 and R56. In total 902 598 archaeal sequences were retrieved, and after quality control and chimera removal steps, 93 %–96 % of the reads were retained (Table S2). A total of 11 different archaeal phyla were identified, and most prevalent phyla were Nanoarchaeota, Micrarchaeota and Crenarchaeota (Table S3). NOPPA15 hosted the most diverse archaeal community ( $H'$  5.97), similar to bacteria (Fig. 5B and Table S2). Most archaeal sequences were affiliated with Nanoarchaeota phylum in NOPPA15, HÄJY30, MIETO17 and HARJA10, with ASVs belonging to *Woesearchaeales* candidate order (74 %, 75 %, 54 %, 40 % relative abundances, respectively) (Figs. 5B and S1b). Bathyarchaea-affiliating archaeal ASVs were also relatively abundant in these samples. *Candidatus* Methanoperedens and *Methanomassiliicoccales*-affiliating ASVs were abundant in HARJA 10 (18 % and 7 % relative abundance, respectively), and in R56 (21 % and 6 %). R56 also had a 11 % relative abundance of *Methanobacterium*, in addition to abundant *Woesearchaeales* (23 %) and Bathyarchaeia (20 %). MIHP15 hosted the least diverse archaeal community ( $H'$  2.05) that differed from other samples (Fig. 5B and Table S2). *Methanoregula*, *Methanobacterium*, and *Methanospirillum*-affiliating ASVs were dominating the ar-

chaeal community in this borehole (50 %, 28 % and 12 % relative abundances, respectively).

Fungal ITS1 amplicon sequencing was successful from the same samples as archaea. Altogether 649 988 sequences were retrieved, but after rigorous quality filtering and chimera removal steps, on average only 41 % of sequences were kept (Table S2). This level was somewhat expected because of high natural length variability of fungal ITS amplicons and typically lower quality of reverse reads that are dropped from the analysis together with their forward pair. Filtering primarily removed low-quality reads and improved the accuracy of ASV inference. According to the Shannon index, the most diverse fungal community was observed in R56 ( $H'$  4.04) and least diverse in MIHP15 ( $H'$  2.22) (Fig. 5C and Table S2). Most of the detected fungal phyla belonged to either Ascomycota or Basidiomycota, and relatively most abundant ASVs affiliated with *Cladosporium* and *Bulleribasidiaceae* (Figs. 5C and S1c). In addition to these, R56 fungal community was composed of *Claviceps* and *Rhodotorula* (8 % and 6 % relative abundances). Fungal communities in NOPPA15, HÄJY30, MIHP15 and MIETO17 all had *Filobasidium*-affiliating ASVs (7 %, 9 %, 5 % and 13 % of the community, respectively). *Itersonilia* affiliating ASV was more typical to HÄJY30 (9 %) than to other samples, and *Melanommataceae*-affiliating ASV was most

relatively most abundant in NOPPA15 (7 %). A large portion (57 %) of the fungal community in HARJA10 could not be identified beyond kingdom-level.

## 4 Discussion

Hydrogeological studies rely on the use of various tracers, most often field measurement data and laboratory analysis of hydrogeochemical parameters, i.e., major ion and trace element concentrations. Natural tracers have been expanded to include the use of different isotopes and microbial communities, in addition to groundwater age tracers such as dissolved gases (e.g., CFCs and SF<sub>6</sub>). These techniques can be used to assess the physical, biological and chemical processes that take place in a hydrogeological setting (Divine and McDonnell, 2005).

### 4.1 The origin and age of groundwater in Kurikka according to tested tracers

Classical hydrogeochemical and isotopic tracers provide the first-order framework for identifying groundwater origin, residence time and degree of mixing in the Kurikka aquifer system. Geochemistry of the sampled water provided initial information about the origin of groundwater in the complex aquifer system in Kurikka. The distinct EC values between unconsolidated aquifer groundwaters (90–204  $\mu\text{S cm}^{-1}$ ) and bedrock groundwater (296  $\mu\text{S cm}^{-1}$ ) indicate different mineralization levels. Higher EC in bedrock groundwater suggests more evolved water, indicating longer residence time allowing for mineral weathering influencing total dissolved solids (TDS). Similarly, the higher pH in bedrock groundwater (8.4), compared to unconsolidated aquifer groundwater (6.2–6.8), is consistent with prolonged water-rock interaction in the bedrock environment and influence of silicate weathering (Frengstad et al., 2001). In deep bedrock environment in Finland, where fluids have retention times of tens of millions of years, groundwaters also have high TDS, EC and pH (Kietäväinen et al., 2013). Major ion composition provided similar characterization of groundwater types. Unconsolidated aquifer groundwater being calcium-bicarbonate (Ca–HCO<sub>3</sub>) or mixed cations–HCO<sub>3</sub> type, and bedrock groundwater being sodium-bicarbonate (Na–HCO<sub>3</sub>) type, indicate different geochemical processes and sources. Often the presence of nitrates and higher chloride levels can indicate anthropogenic influences, such as agriculture, or recent recharge events in groundwater. However, the elevated Cl<sup>–</sup> concentrations observed in bedrock groundwater are more plausibly attributed to prolonged water–rock interaction, rather than anthropogenic inputs, as the relatively thick fine-grained silt layers overlying the Quaternary deposits limit downward transport from the surface (Åberg et al., 2026).

The partial pressure of CO<sub>2</sub> ( $p\text{CO}_2$ ) provides insight into groundwater interaction with soil-derived CO<sub>2</sub> during

recharge (Clark 2015). In water samples from unconsolidated aquifer groundwaters,  $p\text{CO}_2$  values consistently exceeded atmospheric levels (log  $p\text{CO}_2$  over  $-2.0$ ) indicating an open CO<sub>2</sub> system conditions and equilibration with CO<sub>2</sub> produced in the soil zone during infiltration (Appelo and Postma, 2004; Clark, 2015; Freeze and Cherry, 1979). This suggests active exchange between infiltrating groundwater and biologically driven CO<sub>2</sub> in the unsaturated zone, consistent with relatively shallow circulation and ongoing soil–water interaction. In contrast, the lower  $p\text{CO}_2$  observed in bedrock groundwater suggests closed-system conditions, where recharge waters are largely decoupled from the soil zone CO<sub>2</sub> inputs, implying more restricted gas exchange and longer residence times.

The  $\delta^2\text{H}$  and  $\delta^{18}\text{O}$  values from the sampled waters lie on or near the meteoric water lines except for the R56 and MIHP15 samples, that plot, albeit very slightly, above the meteoric water lines. Bedrock groundwater samples may plot above the meteoric water line in the case of prolonged water–rock interaction (Kietäväinen et al., 2013). The longer residence time enables the chemical processes (e.g. silicate hydrolysis) in the water–rock interaction, that can fractionate the isotopic compositions of the water stable isotopes (Kietäväinen et al., 2013). These processes may also explain the MIHP15 water sample plotting slightly above the meteoric water lines, since the MIHP15 well reaches the lowermost aquifer, and most likely has active hydraulic connections to the fractured bedrock below.

The local geology is dominated by crystalline silicate bedrock, including biotite paragneiss, granite, and diorite, which host Rb-bearing silicate minerals. Rubidium-87 (<sup>87</sup>Rb) decays to <sup>87</sup>Sr, and elevated <sup>87</sup>Sr/<sup>86</sup>Sr values may result from felsic mineralogy or silicate weathering that liberates radiogenic strontium inherited from the host rocks (Ikonen et al., 2025; Négrel et al., 2018). The isotopic compositions of strontium in the groundwater samples from the study site vary significantly. Although the bedrock in Kurikka is rich in Rb-bearing mica minerals (biotite and muscovite), which are potential sources of radiogenic strontium, the <sup>87</sup>Sr/<sup>86</sup>Sr ratio in the R56 bedrock groundwater sample was lower than in most unconsolidated aquifer water samples, except for HÄJY30 and MIHP15. This would suggest mixing with groundwater that is enriched in <sup>87</sup>Sr from a different mineralogical locality, or heterogeneity in the geochemistry of the aquifer system. A study conducted in Palmottu, southern Finland, an area with bedrock geology similar to that of Kurikka, reported <sup>87</sup>Sr/<sup>86</sup>Sr values ranging between 0.71999 and 0.75079 in bedrock groundwater samples (Négrel et al., 2003). These values correspond not only to the bedrock groundwater sample R56 in Kurikka, but also to the other samples analysed in this study. If there are hydraulic connections, the mixing of different <sup>87</sup>Sr/<sup>86</sup>Sr end-member waters is the most likely explanation for the varying Sr isotopic compositions in the lower-most unconsolidated aquifer water samples.

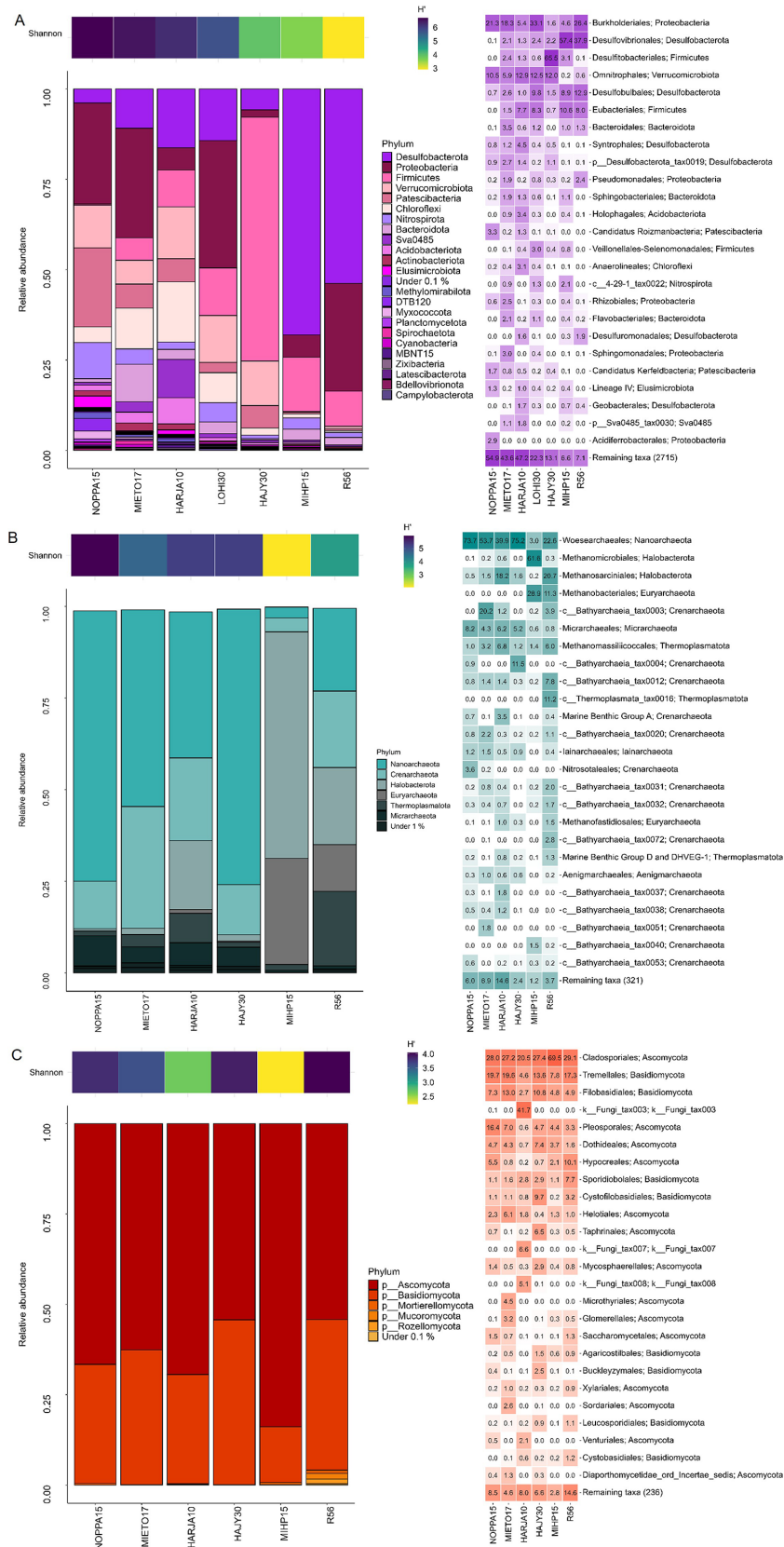


**Figure 5.** Groundwater microbial communities. Bar plots show the relative abundances of different (A) bacterial, (B) archaeal, and (C) fungal phyla and heatmaps represent 25 most abundant orders of (A) bacteria, (B) archaea and (C) fungi.

In a plot of  $^{87}\text{Sr}/^{86}\text{Sr}$  versus the reciprocal Sr concentration ( $1/\text{Sr}^{-1}$ ), binary mixing between end members forms a straight line (Fig. 6). The two dotted lines (red and blue) represent binary mixing trends. The samples near the red dotted mixing line (MIHP15, HÄJY11, MIHP6 and KUU19), represent influence of the Paloluoma and Häjyluoma buried valley modern/young groundwater. The sample points MIHP15 and MIHP6 are located fairly near the Kyrönjoki valley, but the natural flow of groundwater in the Paloluoma valley towards south has a volume that overrides the influence of the larger Kyrönjoki valley groundwater in those sites (Fig. 1). The remaining samples on the blue mixing line (LOHI30, HARJA10 and MIETO17) represent the Kyrönjoki valley groundwater, central part of the buried valley aquifer system, where there is northbound groundwater flow (Fig. 1). The mixing line does not clearly represent this south–north direction, due to hydraulic connections from the large watershed that exists west of LOHI30 (Åberg et al., 2026: Appendix A1; Fig. 3). The sample point NOPPA15 is located north of the buried valley site, and the water sample represents a different geological and geochemical environment representing topmost part of the shallow sedimentary sequence outside the buried valley aquifer system. Therefore, it is most unlikely that there is a hydraulic connection between NOPPA15 and the other sampling sites although it appears as a continuation of the blue mixing line (Fig. 6). R56 and HÄJY30 show non-conservative behaviour outside the two mixing lines. This is most likely explained by bedrock groundwater influence. While R56 is a bedrock groundwater well, HÄJY30 is situated in the most central part of the aquifer system on the bedrock fracture zone, where highly artesian groundwater with heavy outflow character may reflect bedrock groundwater influence creating an additional endmember to the three portrayed in the diagram.

As with the isotopic compositions of strontium the variation in the  $\delta^{34}\text{S}$  values is noticeable (1.1‰–30.3‰). Microbial processes are the most important cause of fractionation for the sulphur isotopes (Canfield, 2001). Due to the microbial reduction of sulphate, the lighter  $^{32}\text{S}$  isotope is removed from the solution (Kaplan and Rittenberg, 1964). A noticeable fractionation of sulphur isotopes can be seen in the samples MIHP15, HÄJY30, HARJA10, R56 and LOHI30 with enriched  $\delta^{34}\text{S}$  values ( $\delta^{34}\text{S} > 12.6$ ). The rest of the samples KUU19, MIETO17, MIHP6 and HÄJY11, ( $\delta^{34}\text{S}$  values 5.3‰–8.8‰), seem to reflect the atmospheric isotopic compositions of sulphur (–5‰ to 10‰) (Clark and Fritz, 1997). In addition, the  $\delta^{34}\text{S}$  value of NOPPA15 stands out, similarly to  $^{87}\text{Sr}/^{86}\text{Sr}$ , in the case of  $\delta^{34}\text{S}$  with a lower isotopic composition and higher sulphur and sulphate concentration to the rest of the samples (Fig. 6). This indicates a sulphur/sulphate source with minimal heavy isotope enrichment and agrees with the microbial community structure with low abundance of sulphate reducers (see Sect. 4.2.1 below). The oxidation-reduction potential in NOPPA15 was close to 0, so neither oxidation nor reduction reactions are

strongly favoured. NOPPA15 water sample had a lighter isotopic composition of sulphur compared to the other samples, suggesting minimal influence from biological processes that typically fractionate sulphur. Furthermore, different mineralogy and water flow paths from the recharge site also probably play a part in the isotope geochemistry in the sampled water from NOPPA15. Thus, NOPPA15 stands out due to its location reflecting a context of a modern esker in the Nenätömänluoma valley (Fig. 1).

Residence time tracers show the presence of a modern water component in four unconsolidated aquifer groundwater locations. This is consistent with a less evolved water type and  $p\text{CO}_2$  values indicative of open-system conditions. In contrast, the only bedrock borehole R56 represents sub-modern water (probably some 10 000 years old, free of CFCs and  $^3\text{H}$ , with the highest  $^4\text{He}_{\text{rad}}$  concentration), with a more evolved water type, and  $p\text{CO}_2$  values reflecting a closed system. The elevated  $^4\text{He}_{\text{rad}}$  concentrations in all samples complicates or prevents the evaluation of groundwater residence times and mixing proportions using the  $^3\text{H}$ – $^3\text{He}$  technique (Shapiro et al., 1998). When radiogenic  $^4\text{He}$  is abundant, accurately separating the tritiogenic helium component becomes challenging and highly uncertain. The use of CFCs as tracers is constrained by their absence, localized contamination (e.g., NOPPA15, KUU19), or microbial degradation by sulphate-reducing microbes in the anoxic conditions of this environment (e.g., HARJA10) (Sonier et al., 1994).

All samples showed  $\text{SF}_6$  concentrations well above solubility equilibrium with modern atmosphere. We concluded that the excessive concentrations are derived from a local natural geogenic source (presence of granite, granodiorite). Similarly, occurrences of extreme  $\text{SF}_6$  values due to natural sources have also been reported in southern Sweden (Åkesson et al., 2015).

While hydrogeochemical parameters, water stable isotopes, strontium, sulfur isotopes and age tracers consistently distinguish between the unconsolidated aquifer and bedrock groundwater, they do not unambiguously resolve mixing proportions or hydraulic connectivity in the area. This ambiguity highlights the limitations of classical tracers alone in highly heterogeneous buried valley systems and motivates the integration of microbial community data, i.e., the microbial fingerprint.

#### 4.2 Hydrogeochemistry is reflected in the microbial community structure of the groundwater

Microbial ecology analyses provide an independent and integrative line of evidence for residence times, groundwater redox conditions, and potential hydraulic connectivity. First, microbial diversity followed roughly the groundwater residence times, supporting the integration of microbial community analysis into a multitracer hydrogeological investigation. Groundwaters with a significant modern recharge component and open system conditions generally hosted more

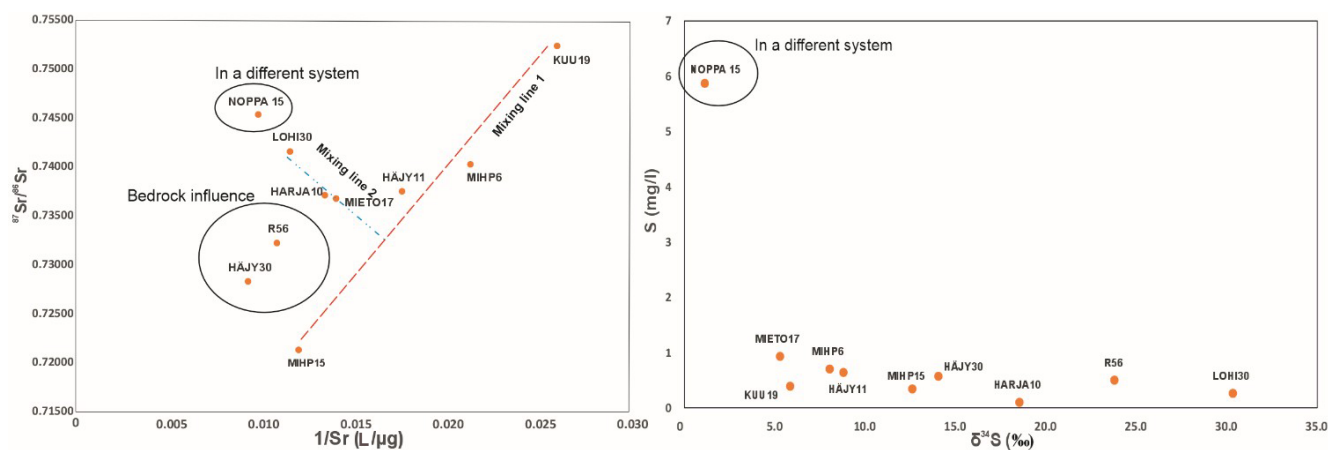


**Figure 6.** On the left  $^{87}\text{Sr}/^{86}\text{Sr}$  values vs. the reciprocal of the Sr concentration with mixing lines (red and blue dotted lines) suggesting several endmembers. NOPPA15 is marked as belonging to a different geochemical environment due to the geology of the area and the characteristics of the groundwater well. Bedrock influence connects the two outliers R56 and HÄJY30. On the right the sulphur concentration vs. the isotopic composition of sulphur ( $\delta^{34}\text{S}$ ) in permille. NOPPA15 marked again as representing a different system.

diverse bacterial and archaeal communities, whereas older and chemically more evolved groundwaters, including the bedrock groundwater, showed lower prokaryotic diversity and dominance of taxa adapted to oligotrophic and energy-limited environments. This pattern is consistent with previous observations that older groundwaters provide fewer and less diverse energy substrates, thereby constraining the microbial diversity (Ben Maamar et al., 2015; Griebler and Lueders, 2009). Although all sampled groundwaters were significantly younger, the diversity indices were approximately at similar level with studies of significantly deeper and older groundwater samples from Fennoscandian bedrock (Kietäväinen et al., 2014; Purkamo et al., 2016). The bedrock groundwater well R56 also hosted a microbial community with a distinct member, *Hydrogenophaga*-affiliating bacteria, which have been detected previously from older groundwaters from Canada (Ruff et al., 2023) and millions of years old, deep drillhole fluids from Fennoscandian bedrock in Finland (e.g., Kietäväinen et al., 2014; Purkamo et al., 2013).

In contrast, fungal communities did not show a consistent relationship with groundwater residence time, suggesting differing ecological controls compared to prokaryotic communities.

Microbial community composition also supported interpretation derived from sulfur isotopes and redox-sensitive geochemical parameters. The analysis method used for analysing the isotopic composition of sulphur from the water samples converts all the sulphur components into sulphate as described in Paris et al. (2013), and sulphide was not analysed separately. With the prevailing conditions of low organic matter, dissolved oxygen levels  $2.7\text{ mg L}^{-1}$  or above, and at least in places high ORP, sulphur in groundwater most likely occurs mainly as sulphate. This supposition is backed by the fact that during field work no sampling site was re-

ported as having the smell of sulphide. Sites with enriched  $\delta^{34}\text{S}$  values (R56, HÄJY30, and MIHP15) hosted substantial populations of sulphate-reducers (e.g., *Desulfovibrio*, *Desulfosporosinus*, *Desulfurivibrio*) indicating active or past microbial sulfate reduction under reducing conditions (Fig. S2). Conversely, groundwater from NOPPA15, characterised by oxic to weakly reducing conditions, low  $\delta^{34}\text{S}$  values and elevated sulfate concentrations, exhibited a low abundance of sulfate reducers, consistent with minimal sulfur isotope fractionation. The coherence between sulfur isotope fractionation and sulfate-reducing microbial abundance demonstrated that microbial data provide support for isotope-based interpretations and help distinguish between geochemical mixing and *in situ* biogeochemical transformation.

Microbes associated with iron cycling were detected in most of the samples, reflecting the prevalence of redox transitions in the aquifer system. The presence of both iron-reducing and iron-oxidizing taxa, including organisms capable of flexible metabolic strategies, like *Rhodospirillum rubrum* (Kato and Ohkuma, 2021) or some Gallionellaceae (Hoover et al., 2023), suggests dynamic and spatially variable redox environments characteristic of buried valley aquifers. At HARJA10, high organic carbon availability appears to favour heterotrophic metabolisms and suppress chemolithoautotrophic iron oxidizers, such as *Gallionella*-type of bacteria using inorganic carbon for growth (Hallbeck and Pedersen, 2014). These observations suggest that iron cycling is locally controlled by carbon availability and redox heterogeneity rather than groundwater age alone.

Carbon cycling within the groundwater system in Kurikka appears to be primarily dominated by heterotrophic fermenters and mixotrophic microorganisms adapted to oligotrophic conditions. Heterotrophic fermenters affiliated with *Candidatus Omnitrophus* (phylum Omnitrophota, formerly

OP3) were abundant across several sites, consistent with their frequent detection and high relative abundance in groundwater environments (Perez-Molphe-Montoya et al., 2022; Suominen et al., 2021; Williams et al., 2021). *Omnitrophales*-affiliating bacteria have been described as a type species from deep underground mine groundwaters (Momper et al., 2017), and are thought to play a central role in mediating carbon cycling, mostly relying on organic carbon fermentation. In addition, some Omnitrophota possess metabolic flexibility, including mixotrophy and ability to utilize the Wood-Ljungdahl pathway to carbon dioxide fixation and acetate production (Perez-Molphe-Montoya et al., 2022). A high relative abundance of *Omnitrophus* was also observed in samples with elevated Sr concentrations and detectable chromium concentrations is consistent with previous studies showing dominant *Omnitrophales* or *Verrucomicrobiota* in environments with enriched elevated concentrations of these trace metals (Bärenstrauch et al., 2022; Zhang et al., 2021).

Patescibacteria-affiliating ASVs were prevalent in groundwater prokaryotic communities observed in this study, consistent with previous studies (Lyons et al., 2021; Schwab et al., 2017). Their streamlined genomes and limited biosynthetic capabilities suggest a primarily fermentative metabolism and strong dependence on metabolic interactions with other community members (Bärenstrauch et al., 2022; Chaudhari et al., 2021; Luef et al., 2015). The frequent co-occurrence of Patescibacteria, Omnitrophota and Nitrospirata, as was the case in the Kurikka aquifer system, indicates networking and potential syntrophic dependencies between these microbial components of the community, potentially facilitating organic carbon degradation and recycling under energy-limited conditions, as proposed in previous studies (Chaudhari et al., 2021).

Archaeal communities further reinforce the importance of fermentation-based carbon cycling in Kurikka groundwater. Archaeal assemblages were dominated by Woesearchaeales, which are commonly detected from groundwater environments and are believed to rely on fermentation-based metabolisms under anoxic conditions (Castelle et al., 2015; Liu et al., 2018). Similarly, other dominant group Bathyarchaeia, have been associated with complex organic matter degradation and fermentative lifestyle (Hou et al., 2025).

The combined dominance of fermentative bacteria and archaea, together with the presence of homoacetogenic microorganisms, indicates somewhat internally sustained carbon cycle within the aquifer system. Acetate produced through fermentation and homoacetogenesis can serve as a central intermediate, supporting not only heterotrophic microbes but also sulphate reducing community by providing a continuous source of suitable substrate for energy and growth (Lever, 2012).

Despite the limited understanding of fungal metabolic capabilities in groundwater systems (Retter et al., 2024), most taxa identified here belong to saprotrophic lineages that are

typically adapted to oligotrophic conditions. It is likely that the fungal communities in Kurikka sites are originating from surface environments, as many taxa are associated with soil, plant litter or phyllosphere inputs (Retter et al., 2024) and are distinct from the deeper bedrock groundwater communities described previously (Purkamo et al., 2018; Sohlberg et al., 2015). The observation of microbial communities with versatile carbon metabolism strategies supports a subsurface carbon cycle capable of sustaining microbial activity in these energy-limited groundwater environments.

Nitrogen-cycling microorganisms, particularly Nitrospirae-related taxa, were detected mainly under hypoxic to anoxic conditions, and the detected Nitrospirata lineages here showed similarities with the findings of Mosley et al. (2024), showing that the majority of Nitrospirata genomes recovered from aquifers possess metabolic traits linked to anaerobic nitrogen and sulphur. Other recent studies highlight the importance of Nitrospirae in groundwater ecosystems and their diverse metabolic abilities (Mosley et al., 2024; Poghosyan et al., 2019; Schwab et al., 2017). The distribution of these taxa further reflects advanced, post-denitrification redox conditions and supports the interpretation that nitrogen transformations pathways in the aquifer are shaped primarily by oxygen availability and groundwater residence time.

Low biomass in groundwater samples resulted in very small amounts of recoverable DNA, which is the probable cause for unsuccessful retrieval of sequencing data from KUU19, MIHP6 and HÄJY11. Additionally, only bacterial community from LOHI30 could be retrieved. Archaea are typically less abundant in groundwater environments compared to bacteria, and with low amount of DNA to begin with here, sequencing has missed the archaea. Similarly, the abundance of fungal cells in groundwaters might be much lower than bacteria, and additionally, fungi may also require more rigorous cell-disruption steps during extraction compared to prokaryotes, causing a reduced fungal DNA yield and unsuccessful sequencing here. In addition, the filters used here were not specifically designed for this purpose, so methodological limitations may have led to inefficient biomass elution and low final DNA recovery. One potential reason for low DNA recovery could also be organic compounds interfering with the DNA extraction, as we detected a brownish colour emerging to the filters while pumping the groundwater through.

Overall, microbial community structure provides mechanistic support for hydrogeochemical and isotopic interpretations and helps distinguish between groundwater mixing and in situ biogeochemical transformation in this complex buried valley aquifer system.

### 4.3 Usability of tested tracers in complex aquifers

The tracers applied in this study provide valuable initial insights into the Kurikka buried valley aquifer system and

demonstrate their potential for supporting further hydrogeological characterization, even though some limitations were identified. Despite the challenges brought by observation wells with long screens (12–30 m) and single-campaign sampling, the combination of isotopic, residence time and microbial approaches produced a broad and informative view of groundwater processes in a geologically complex setting.

Water stable isotopes proved effective in establishing that sampled groundwaters do not contain a surface water component. Their clear and consistent signatures form a robust baseline for tracing future hydraulic changes influenced by extensive groundwater extraction. Although spatial variability exists, strontium isotope signatures provide an important reference for identifying mixing of groundwaters in the Kurikka buried valley aquifer system as pumping tests continue and more sampling campaigns are carried out.

This single-campaign study excludes the seasonal changes in redox conditions that might affect the S isotopic compositions, or the seasonal changes in the isotopic compositions of water stable isotopes in precipitation. Furthermore, the sampling was done from only 10 locations. For a more complete hydrogeochemical assessment of the end-member compositions more sampling around the study area can be recommended and will be published as results of the additional hydrogeological investigations of the study area.

The applicability of different environmental tracers for groundwater age dating was assessed in this study. While CFCs, noble gases and SF<sub>6</sub> were rendered unreliable by tracer degradation, contamination, excess air and in-situ production process, the <sup>3</sup>H–<sup>3</sup>He method yielded robust age estimates for selected samples, despite elevated radiogenic helium concentrations. These results underline the need for site-specific tracer assessment and confirm that meaningful groundwater residence times can be derived even in complex hydrogeological settings. An advantage would be observation wells with short filter screen of for example ~ 2 m. Tritium with low detection limit, achievable with the <sup>3</sup>He ingrowth method, as well as radiocarbon emerge as promising options for improving residence time estimates and identification of old groundwater components in the system.

Microbial community profiling revealed differences between the sites. However, many phyla and orders are shared among all sites, this taxonomic overlap limits their use as standalone tracers. Greater resolution might be achieved by examining lower taxonomic levels, and while partial 16S rRNA gene sequencing typically lacks species-level accuracy (Johnson et al., 2019), this can be circumvented by sequencing the whole 16S rRNA gene using long-read approaches. Specific taxa, such as *Hydrogenophaga*, show promise as indicators of specific environments like bedrock groundwater. The microbial community diversity also tracked well with groundwater age, supporting their use as complementary tracers of subsurface environments.

## 5 Conclusions and Implications

This study highlighted the unique characteristics of deep groundwaters found in the buried valley aquifer system in Kurikka, focusing on combined isotopic, residence time and microbial tracer analyses. Together, these approaches provide a robust, first-order understanding of the groundwater system structure, connectivity and functioning prior to extensive groundwater extraction. The findings indicate that the groundwater in the Paloluoma Valley and Harjankylä in the Kyrönjoki Valley appear to be younger compared to the other areas in the Kyrönjoki Valley. This is attributed to the proximity of recharge areas, an important observation for groundwater management, as it indicates areas where the system may respond more rapidly to pumping and seasonal variations. Isotopic compositions of oxygen and hydrogen confirm that no surface water component is present in the groundwater samples. Strontium isotopes reflect local mineralogy and establish a reference for future mixing studies, assuming the pumping tests will influence the hydraulic connections in the aquifer system. Isotopic evidence suggests hydraulic connectivity between the lowermost aquifer and the underlying fractured bedrock. Although the extent of the fractured bedrock as a water reservoir remains unclear, the isotope data indicate that interactions between the two units are likely. The study shows that several environmental tracers for groundwater residence time determination fail under the investigated conditions. However, the <sup>3</sup>H–<sup>3</sup>He method remained applicable for samples with measurable <sup>3</sup>H. Groundwater residence time estimates indicate predominantly modern water. This further supports the interpretation that where mixing occurs between water from the bedrock surface and the lowermost unconsolidated aquifer, the groundwater flow within the fractured bedrock is likely relatively unrestricted.

The results demonstrate that groundwater microbial communities are diverse and vary distinctly between the studied sites along the aquifer system in Kurikka. The bedrock-related microbial community exhibits special features compared to the groundwaters from shallower unconsolidated aquifers. The site at a more superficial esker system with relatively young groundwater hosted the most diverse prokaryotic community, whereas bedrock with the oldest waters supported the lowest diversity. This age-dependent trend is consistent with geochemical expectations for deep, isolated groundwater environments.

Sulphur isotope compositions in the groundwater further reinforce the link between geochemistry and microbiology.

Because this study was conducted prior to large-scale groundwater extraction, the geochemical, isotopic, residence time and microbial data presented here form an essential baseline. Thus, each sampling site can serve as an endmember against which future changes can be evaluated. Establishing these initial conditions is important for detecting shifts in e.g., geochemical pathways or microbial activity that may arise as the aquifer system responds to stress.

Although one of the aims of this study was to assess whether a combined multitracer approach could resolve hydraulic connectivity and flow dynamics within this complex buried valley system, the present dataset provides only preliminary indications rather than definitive evidence. Isotopic, microbial and sulphur-isotope patterns point to potential zones of interaction between aquifer units, but limitations in spatial coverage, well construction and temporal resolution prevent firm conclusions regarding flow paths or mixing processes. Instead, the results identify where such connections may exist and highlight which tracers are most promising for future high-resolution investigations. The multitracer framework establishes the methodological foundation for future studies designed to rigorously test this hypothesis under expanded sampling and pumping conditions. Although the dataset is limited, the results demonstrate that integrating microbial community structure with classical hydrogeochemical and isotopic tracers improves interpretation of groundwater connectivity and biogeochemical processes compared to using conventional tracers alone.

Further research is still required to clarify outstanding questions, including the extent of hydraulic conductivity between different parts of the aquifer and the fractured bedrock underneath, and its role as a potential flow path. Nonetheless, the insights gained here provide a foundation for understanding and managing groundwater resources. These results serve as key references for interpreting test pumping data and future investigations in the unique Kurikka buried valley aquifer system.

*Data availability.* All data is available either in the publication, in its Supplement, or NCBI's SRA (<https://www.ncbi.nlm.nih.gov/sra/?term=PRJNA1270735>, NIH, 2026) under BioProject PRJNA1270735 (sequence data).

*Supplement.* The supplement related to this article is available online at <https://doi.org/10.5194/bg-23-4463-2026-supplement>.

*Author contributions.* LP, JI and M-AP jointly conceptualized the idea, conducted the investigation, analysed the data and wrote and edited the original manuscript. NP took part in conceptualization, provided funding and resources and commented on the original manuscript. JS took part in investigation and participated in the revision of the manuscript. MM took part in investigation and commented on the original manuscript. A-MH took part in conceptualization, investigation and analysis of the data and writing and editing of the original manuscript. TP provided resources and participated in conceptualization of the idea. ITM provided funding and resources and mentoring during idea conceptualization.

*Competing interests.* The contact author has declared that none of the authors has any competing interests.

*Disclaimer.* Publisher's note: Copernicus Publications remains neutral with regard to jurisdictional claims made in the text, published maps, institutional affiliations, or any other geographical representation in this paper. The authors bear the ultimate responsibility for providing appropriate place names. Views expressed in the text are those of the authors and do not necessarily reflect the views of the publisher.

*Acknowledgements.* Arto Pullinen, Salla Valpola, Vaula Lukkariinen and Kim Wennman are thanked for their help during the fieldwork. Yann Lahaye, Mia Tiljander, Meiru Zhou and Katariina Issukka at the GTK laboratory, and the personnel of laboratory of water microbiology at THL are acknowledged for their contribution to laboratory analyses. Nina Hendriksson and Aleksu Tuunainen are thanked for the helpful comments and aid with the characteristics of groundwater wells. Authors also thank the Kurikka Aquifer project consortium partners: Kurikka Vesihuolto Oy, Vaasan Vesi, and ELY Centre for South Ostrobothnia (EPOELY) for funding and resources for the project. We are also sincerely thankful to all private landowners who allowed access to the sampling sites. During the preparation of this manuscript the authors used Microsoft Copilot to improve language and readability. After using this tool, the authors reviewed and edited the content as needed and take full responsibility for the content of the publication.

*Review statement.* This paper was edited by Mark Lever and reviewed by four anonymous referees.

## References

- Åberg, A. K., Korkka-Niemi, K., Åberg, S. C., and Rautio, A.: Application of 3D hydrogeochemistry and particle tracking in detecting groundwater flow patterns within an aapa mire-outwash plain system in a boreal environment at a mining development site, *Appl. Geochem.*, 186, 106360, <https://doi.org/10.1016/j.apgeochem.2025.106360>, 2025.
- Åberg, A. K., Putkinen, N., Eyles, N., Davidila, J., and Malinowski, M.: 3D hydrostratigraphic architecture of a Late Pleistocene buried valley infill at Kurikka, west-central Finland, *Quatern. Int.*, 755, <https://doi.org/10.1016/j.quaint.2025.110080>, 2026.
- Åkesson, M., Suckow, A., Visser, A., Sültenfuss, J., Laier, T., Purtschert, R., and Sparrenbom, C. J.: Constraining age distributions of groundwater from public supply wells in diverse hydrogeological settings in Scania, Sweden, *J. Hydrol.*, 528, <https://doi.org/10.1016/j.jhydrol.2015.06.022>, 2015.
- Abarenkov, K., Nilsson, R. H., Larsson, K. H., Taylor, A. F. S., May, T. W., Frøslev, T. G., Pawlowska, J., Lindahl, B., Pöldmaa, K., Truong, C., Vu, D., Hosoya, T., Niskanen, T., Piirmann, T., Ivanov, F., Zirk, A., Peterson, M., Cheeke, T. E., Ishigami, Y., Jansson, A. T., Jeppesen, T. S., Kristiansson, E., Mikryukov, V., Miller, J. T., Oono, R., Ossandon, F. J., Paupério, J., Saar, I., Schigel, D., Suija, A., Tedersoo, L., and Kõljalg, U.: The UNITE database for molecular identification and taxonomic communication of fungi and other eukaryotes: sequences, taxa and classification

- cations reconsidered, *Nucleic Acids Res.*, 52, D791–D797, <https://doi.org/10.1093/NAR/GKAD1039>, 2024.
- Andersen, K. S., Kirkegaard, R. H., Karst, S. M., and Albertsen, M.: ampvis2: an R package to analyse and visualise 16S rRNA amplicon data, <https://doi.org/10.1101/299537>, 11 April 2018.
- Appelo, C. A. J. and Postma, D.: *Geochemistry, groundwater and pollution*, 2nd edn., Geochemistry, Groundw. Pollution, 1–649, <https://doi.org/10.1201/9781439833544>, 2004.
- Apprill, A., McNally, S., Parsons, R., and Weber, L.: Minor revision to V4 region SSU rRNA 806R gene primer greatly increases detection of SAR11 bacterioplankton, *Aquat. Microb. Ecol.*, 75, 129–137, <https://doi.org/10.3354/ame01753>, 2015.
- Ben Maamar, S., Aquilina, L., Quaiser, A., Pauwels, H., Michon-Coudouel, S., Vergnaud-Ayraud, V., Labasque, T., Roques, C., Abbott, B. W., and Dufresne, A.: Groundwater isolation governs chemistry and microbial community structure along hydrologic flowpaths, *Front. Microbiol.*, 6, 1–13, <https://doi.org/10.3389/fmicb.2015.01457>, 2015.
- Bärenstrauch, M., Vanhove, A. S., Allégra, S., Peuble, S., Gallice, F., Paran, F., Lavastre, V., and Girardot, F.: Microbial diversity and geochemistry of groundwater impacted by steel slag leachates, *Sci. Total Environ.*, 843, 156987, <https://doi.org/10.1016/J.SCITOTENV.2022.156987>, 2022.
- Callahan, B. J., McMurdie, P. J., Rosen, M. J., Han, A. W., Johnson, A. J. A., and Holmes, S. P.: DADA2: High resolution sample inference from Illumina amplicon data, *Nat. Methods*, 13, 581, <https://doi.org/10.1038/NMETH.3869>, 2016.
- Canfield, D. E.: Biogeochemistry of sulfur isotopes, *Rev. Mineral. Geochem.*, 43, <https://doi.org/10.2138/gsrmg.43.1.607>, 2001.
- Carreira, P. M. and Marques, J. M.: The Use of Environmental Isotopes in Hydrogeology, *Water*, 16, 914, <https://doi.org/10.3390/w16070914>, 2024.
- Castelle, C. J., Wrighton, K. C., Thomas, B. C., Hug, L. A., Brown, C. T., Wilkins, M. J., Frischkorn, K. R., Tringe, S. G., Singh, A., Markillie, L. M., Taylor, R. C., Williams, K. H., and Banfield, J. F.: Genomic expansion of domain archaea highlights roles for organisms from new phyla in anaerobic carbon cycling, *Curr. Biol.*, 25, 690–701, <https://doi.org/10.1016/j.cub.2015.01.014>, 2015.
- Cauquoin, A., Fourré, Landais, A., Okazaki, A., and Yoshimura, K.: Modeling Natural Tritium in Precipitation and its Dependence on Decadal Solar Activity Variations Using the Atmospheric General Circulation Model MIROC5-Iso, *J. Geophys. Res.-Atmos.*, 129, <https://doi.org/10.1029/2023JD039745>, 2024.
- Chaudhari, N. M., Overholt, W. A., Figueroa-Gonzalez, P. A., Taubert, M., Bornemann, T. L. V., Probst, A. J., Hölzer, M., Marz, M., and Küsel, K.: The economical lifestyle of CPR bacteria in groundwater allows little preference for environmental drivers, *Environ. Microbiomes*, 16, 1–18, <https://doi.org/10.1186/s40793-021-00395-w>, 2021.
- Clark, I.: *Groundwater geochemistry and isotopes*, CRC press, Taylor and Francis Group, Boca Raton, FL, US, 438 p., <https://doi.org/10.1201/b18347>, 2015.
- Clark, I. and Fritz, P.: *Environmental Isotopes in Hydrogeology*, CRC press, Taylor and Francis Group, Boca Raton, FL, US, 328 p., <https://doi.org/10.1201/B18347>, 1997.
- Cloutier, V., Lefebvre, R., Savard, M. M., Bourque, É., and Therrien, R.: Hydrogeochemistry and groundwater origin of the Basses-Laurentides sedimentary rock aquifer system, St. Lawrence Lowlands, Québec, Canada, *Hydrogeol. J.*, 14, <https://doi.org/10.1007/s10040-005-0002-3>, 2006.
- Cook, P. G. and Solomon, D. K.: Recent advances in dating young groundwater: Chlorofluorocarbons,  $^3\text{H}/^3\text{He}$  and  $^{85}\text{Kr}$ , *J. Hydrol.*, 191, [https://doi.org/10.1016/S0022-1694\(96\)03051-X](https://doi.org/10.1016/S0022-1694(96)03051-X), 1997.
- de Vries A. and Ripley, B. D.: gg dendro: Create Dendrograms and Tree Diagrams Using “ggplot2”, R package version 0.2.0, <https://andrie.github.io/ggdendro/> (last access: 17 November 2025), 2024.
- Divine, C. E. and McDonnell, J. J.: The future of applied tracers in hydrogeology, *Hydrogeol. J.*, 13, <https://doi.org/10.1007/s10040-004-0416-3>, 2005.
- Freeze, R. A. and Cherry, J. A.: *Groundwater*, Prentice-Hall, Englewood Cliffs, 604 p., ISBN 9780133653120, 1979.
- Frengstad, B., Banks, D., and Siewers, U.: The chemistry of Norwegian groundwaters: IV. The pH-dependence of element concentrations in crystalline bedrock groundwaters, *Sci. Total Environ.*, 277, 101–117, [https://doi.org/10.1016/S0048-9697\(00\)00867-6](https://doi.org/10.1016/S0048-9697(00)00867-6), 2001.
- Gantner, S., Andersson, A. F., Alonso-Sáez, L., and Bertilsson, S.: Novel primers for 16S rRNA-based archaeal community analyses in environmental samples, *J. Microbiol. Meth.*, 84, 12–18, <https://doi.org/10.1016/j.mimet.2010.10.001>, 2011.
- Griebler, C. and Lueders, T.: Microbial biodiversity in groundwater ecosystems, *Freshwater Biol.*, 54, 649–677, <https://doi.org/10.1111/j.1365-2427.2008.02013.x>, 2009.
- Grönwall, J. and Danert, K.: Regarding groundwater and drinking-water access through a human rights lens: Self-Supply as a norm, *Water (Switzerland)*, 12, <https://doi.org/10.3390/w12020419>, 2020.
- Hall, A. M., Putkinen, N., Hietala, S., Lindsberg, E., and Holma, M.: Ultra-slow cratonic denudation in Finland since 1.5 Ga indicated by tiered unconformities and impact structures, *Precambrian Res.*, 352, 106000, <https://doi.org/10.1016/J.PRECAMRES.2020.106000>, 2021.
- Hallbeck, L. and Pedersen, K.: The family Gallionellaceae, in: *The Prokaryotes: Alphaproteobacteria and Betaproteobacteria*, edited by: Rosenberg, E., DeLong, E. F., Lory, S., Stackebrandt, E., and Thompson, F., Springer, Berlin, 853–858, [https://doi.org/10.1007/978-3-642-30197-1\\_398](https://doi.org/10.1007/978-3-642-30197-1_398), 2014.
- Harrison, A. G. and Thode, H. G.: Sulphur Isotope Abundances in Hydrocarbons and Source Rocks of Uinta Basin, Utah, *Am. Assoc. Petr. Geol. B.*, 42, <https://doi.org/10.1306/0bda5c00-16bd-11d7-8645000102c1865d>, 1958.
- Herlemann, D. P., Labrenz, M., Jürgens, K., Bertilsson, S., Waniek, J. J., and Andersson, A. F.: Transitions in bacterial communities along the 2000 km salinity gradient of the Baltic Sea, *ISME J.*, 5, 1571–1579, <https://doi.org/10.1038/ismej.2011.41>, 2011.
- Hoover, R. L., Keffer, J. L., Polson, S. W., and Chan, C. S.: Gallionellaceae pangenomic analysis reveals insight into phylogeny, metabolic flexibility, and iron oxidation mechanisms, *mSystems*, 8, [https://doi.org/10.1128/MSYSTEMS.00038-23/SUPPL\\_FILE/MSYSTEMS.00038-23-S0002.XLSX](https://doi.org/10.1128/MSYSTEMS.00038-23/SUPPL_FILE/MSYSTEMS.00038-23-S0002.XLSX), 2023.
- Hou, J., Yang, C., and Wang, F.: Carbon metabolic versatility underpins Bathyarchaea ecological significance across the global deep subsurface, *ISME J.*, 19, 259, <https://doi.org/10.1093/ISMEJO/WRAF259>, 2025.

- Ikonen, J., Rauhala, A., Tuomela, A., Postila, H., Kumpula, T., Korpelainen, P., Pietilä, R., Valtta, R. O., Lerssi, J., Panttila, H., and Korkka-Niemi, K.: Combining UAS-TIR and GEM-2 Techniques for Focused Water Sampling and Isotope Geochemical Analysis at Two Mine Sites in Northern Finland, *Mine Water Environ.*, 44, <https://doi.org/10.1007/s10230-024-01020-1>, 2025.
- Inkinen, J., Jayaprakash, B., Siponen, S., Hokajärvi, A. M., Pursiainen, A., Ikonen, J., Ryzhikov, I., Täubel, M., Kauppinen, A., Paananen, J., Miettinen, I. T., Torvinen, E., Kolehmainen, M., and Pitkänen, T.: Active eukaryotes in drinking water distribution systems of ground and surface waterworks, *Microbiome*, 7, 1–17, <https://doi.org/10.1186/S40168-019-0715-5>, 2019.
- Jaunat, J., Huneau, F., Dupuy, A., Celle-Jeanton, H., Vergnaud-Ayraud, V., Aquilina, L., Labasque, T., and Le Coustumer, P.: Hydrochemical data and groundwater dating to infer differential flowpaths through weathered profiles of a fractured aquifer, *Appl. Geochem.*, 27, <https://doi.org/10.1016/j.apgeochem.2012.06.009>, 2012.
- Johnson, J. S., Spakowicz, D. J., Hong, B. Y., Petersen, L. M., Demkowicz, P., Chen, L., Leopold, S. R., Hanson, B. M., Agresta, H. O., Gerstein, M., Sodergren, E., and Weinstock, G. M.: Evaluation of 16S rRNA gene sequencing for species and strain-level microbiome analysis, *Nat. Commun.*, 10, 1–11, <https://doi.org/10.1038/s41467-019-13036-1>, 2019.
- Johnson, T. D., Belitz, K., Kauffman, L. J., Watson, E., and Wilson, J. T.: Populations using public-supply groundwater in the conterminous U. S. 2010; Identifying the wells, hydrogeologic regions, and hydrogeologic mapping units, *Sci. Total Environ.*, 806, <https://doi.org/10.1016/j.scitotenv.2021.150618>, 2022.
- Kaislaniemi, L.: Estimating the distribution of strontium isotope ratios  $^{87}\text{Sr}/^{86}\text{Sr}$  in the Precambrian of Finland, *Bull. Geol. Soc. Finl.*, 83, <https://doi.org/10.17741/bgsf/83.2.002>, 2011.
- Kaplan, I. R. and Rittenberg, S. C.: Microbiological fractionation of sulphur isotopes, *J. Gen. Microbiol.*, 34, 195–212, <https://doi.org/10.1099/00221287-34-2-195>, 1964.
- Kato, S. and Ohkuma, M.: A Single Bacterium Capable of Oxidation and Reduction of Iron at Circumneutral pH, *Microbiol. Spectr.*, 9, [https://doi.org/10.1128/SPECTRUM.00161-21/SUPPL\\_FILE/SPECTRUM00161-21\\_SUPP\\_1\\_SEQ4.PDF](https://doi.org/10.1128/SPECTRUM.00161-21/SUPPL_FILE/SPECTRUM00161-21_SUPP_1_SEQ4.PDF), 2021.
- Kauppinen, A., Pitkänen, T., Al-Hello, H., Maunula, L., Hokajärvi, A. M., Rimhanen-Finne, R., and Miettinen, I. T.: Two Drinking Water Outbreaks Caused by Wastewater Intrusion Including Sapovirus in Finland, *Int. J. Env. Res. Pub. He.*, 16, 4376, <https://doi.org/10.3390/IJERPH16224376>, 2019.
- Kietäväinen, R., Ahonen, L., Kukkonen, I. T., Hendriksson, N., Nyssönen, M., and Itävaara, M.: Characterisation and isotopic evolution of saline waters of the Outokumpu Deep Drill Hole, Finland—Implications for water origin and deep terrestrial biosphere, *Appl. Geochem.*, 32, 37–51, <https://doi.org/10.1016/j.apgeochem.2012.10.013>, 2013.
- Kietäväinen, R., Ahonen, L., Kukkonen, I. T., Niedermann, S., Wiersberg, T., Kietäväinen, R., Ahonen, L., Kukkonen, I. T., Niedermann, S., Wiersberg, T., Kieta, R., Ahonen, L., Kukkonen, I. T., Niedermann, S., and Wiersberg, T.: Noble gas residence times of saline waters within crystalline bedrock, Outokumpu Deep Drill Hole, Finland, *Geochim. Cosmochim. Ac.*, 145, 159–174, <https://doi.org/10.1016/j.gca.2014.09.012>, 2014.
- Kipfer, R., Aeschbach-Hertig, W., Peeters, F., and Stute, M.: Noble gases in lakes and ground waters, *Rev. Mineral Geochem.*, 47, <https://doi.org/10.2138/rmg.2002.47.14>, 2002.
- Kløve, B., Kvitsand, H. M. L., Pitkänen, T., Gunnarsdottir, M. J., Gaut, S., Gardarsson, S. M., Rossi, P. M., and Miettinen, I.: Overview of groundwater sources and water-supply systems, and associated microbial pollution, in Finland, Norway and Iceland, *Hydrogeol. J.*, 25, 1033–1044, <https://doi.org/10.1007/s10040-017-1552-x>, 2017.
- Lahermo, P., Ilmasti, M., Juntunen, R., and Taka, M.: The hydrogeochemical mapping of Finnish groundwater = Suomen geokemian atlas. Osa 1: Suomen pohjavesien hydrokemiallinen kartoitus, Geologian tutkimuskeskus, Espoo, 66 p., ISBN 9516903746, 1990.
- Lahtinen, R., Huhma, H., Sipilä, P., and Vaarma, M.: Geochemistry, U–Pb geochronology and Sm–Nd data from the Paleoproterozoic Western Finland supersuite – A key component in the coupled Bothnian oroclinal, *Precambrian Res.*, 299, 264–281, <https://doi.org/10.1016/J.PRECAMRES.2017.07.025>, 2017.
- Lee, J. H., Lee, B. J., and Unno, T.: Bacterial Communities in Ground-and Surface Water Mixing Zone Induced by Seasonal Heavy Extraction of Groundwater, *Geomicrobiol. J.*, 35, 768–774, <https://doi.org/10.1080/01490451.2018.1468834>, 2018.
- Lever, M. A.: Acetogenesis in the energy-starved deep biosphere – a paradox?, *Front. Microbiol.*, 2, 284, <https://doi.org/10.3389/fmicb.2011.00284>, 2012.
- Liu, X., Li, M., Castelle, C. J., Probst, A. J., Zhou, Z., Pan, J., Liu, Y., Banfield, J. F., and Gu, J. D.: Insights into the ecology, evolution, and metabolism of the widespread Woese archaeotal lineages, *Microbiome*, 6, 102, <https://doi.org/10.1186/s40168-018-0488-2>, 2018.
- Luef, B., Frischkorn, K. R., Wrighton, K. C., Holman, H. N., Birarda, G., Thomas, B. C., Singh, A., Williams, K. H., Siegerist, C. E., Tringe, S. G., Downing, K. H., Comolli, L. R., and Banfield, J. F.: Diverse uncultivated ultra-small bacterial cells in groundwater, *Nat. Commun.*, 6, 1–8, <https://doi.org/10.1038/ncomms7372>, 2015.
- Luoma, S., Majaniemi, J., Pullinen, A., Mursu, J., and Virtasalo, J. J.: Geological and groundwater flow model of a submarine groundwater discharge site at Hanko (Finland), northern Baltic Sea, *Hydrogeol. J.*, 29, 1279–1297, <https://doi.org/10.1007/s10040-021-02313-3>, 2021.
- Luoma, S., Okkonen, J., Korkka-Niemi, K., Hendriksson, N., and Paalijärvi, M.: Characterization of Groundwater Geochemistry in an Esker Aquifer in Western Finland Based on Three Years of Monitoring Data, *Water (Switzerland)*, 16, <https://doi.org/10.3390/w16223301>, 2024.
- Lyons, K. J., Hokajärvi, A.-M., Ikonen, J., Kauppinen, A., Miettinen, I. T., Pitkänen, T., Rossi, P. M., and Kujala, K.: Surface Water Intrusion, Land Use Impacts, and Bacterial Community Composition in Shallow Groundwater Wells Supplying Potable Water in Sparsely Populated Areas of a Boreal Region, *Microbiology Spectrum*, 9, e00179-21, <https://doi.org/10.1128/Spectrum.00179-21>, 2021.
- Martin, M.: Cutadapt removes adapter sequences from high-throughput sequencing reads, *EMBnet. J.*, 17, 10–12, <https://doi.org/10.14806/EJ.17.1.200>, 2011.
- Massmann, G., Sültenfuß, J., Dünnbier, U., Knappe, A., Taute, T., and Pekdeger, A.: Investigation of groundwater residence times

- during bank filtration in Berlin: A multi-tracer approach, *Hydrol. Process.*, 22, <https://doi.org/10.1002/hyp.6649>, 2008.
- Mayer, A., Sültenfuß, J., Travi, Y., Rebeix, R., Purtschert, R., Claude, C., Le Gal La Salle, C., Miche, H., and Conchetto, E.: A multi-tracer study of groundwater origin and transit-time in the aquifers of the Venice region (Italy), *Appl. Geochem.*, 50, <https://doi.org/10.1016/j.apgeochem.2013.10.009>, 2014.
- McMurdie, P. J. and Holmes, S.: Phyloseq: An R Package for Reproducible Interactive Analysis and Graphics of Microbiome Census Data, *PLoS One*, 8, <https://doi.org/10.1371/journal.pone.0061217>, 2013.
- Merino, N., Jackson, T. R., Campbell, J. H., Kersting, A. B., Sackett, J., Fisher, J. C., Bruckner, J. C., Zavarin, M., Hamilton-Brehm, S. D., and Moser, D. P.: Subsurface microbial communities as a tool for characterizing regional-scale groundwater flow, *Sci. Total Environ.*, 842, 156768, <https://doi.org/10.1016/j.scitotenv.2022.156768>, 2022.
- Meyzonnat, G., Musy, S., Corcho-Alvarado, J. A., Barbecot, F., Pinti, D. L., Purtschert, R., Lauzon, J. M., and McCormack, R.: Age distribution of groundwater in fractured aquifers of the St. Lawrence Lowlands (Canada) determined by environmental tracers ( $^3\text{H}/^3\text{He}$ ,  $^{85}\text{Kr}$ ,  $\text{SF}_6$ , CFC-12,  $^{14}\text{C}$ ), *Hydrogeol. J.*, 31, <https://doi.org/10.1007/s10040-023-02671-0>, 2023.
- Momper, L., Jungbluth, S. P., Lee, M. D., and Amend, J. P.: Energy and carbon metabolisms in a deep terrestrial subsurface fluid microbial community, *ISME J.*, 11, 2319–2333, <https://doi.org/10.1038/ismej.2017.94>, 2017.
- Mosley, O. E., Gios, E., and Handley, K. M.: Implications for nitrogen and sulphur cycles: phylogeny and niche-range of Nitrospirota in terrestrial aquifers, *ISME Commun.*, 4, 47, <https://doi.org/10.1093/ISMECO/YCAE047>, 2024.
- National Ground Water Association: <https://www.ngwa.org/what-is-groundwater/About-groundwater>, last access: 1 April 2025.
- Négre, P., Casanova, J., Blomqvist, R., Kaija, J., and Frape, S.: Strontium isotopic characterization of the Palmottu hydro-system (Finland): Water-rock interaction and geochemistry of groundwaters, *Geofluids*, 3, <https://doi.org/10.1046/j.1468-8123.2003.00056.x>, 2003.
- Négre, P., Pauwels, H., and Chabaux, F.: Characterizing multiple water-rock interactions in the critical zone through Sr-isotope tracing of surface and groundwater, *Appl. Geochem.* 93, 102–112, <https://doi.org/10.1016/j.apgeochem.2018.04.006>, 2018.
- NIH: SRA – PRJNA1270735, NIH [data set], <https://www.ncbi.nlm.nih.gov/sra/?term=PRJNA1270735> (last access: 2 July 2026), 2026.
- Oksanen, J., Simpson, G. L., Blanchet, F. G., Kindt, R., Legendre, P., Minchin, P. R., O'Hara, R. B., Solymos, P., Stevens, M. H. H., Szoecs, E., Wagner, H., Barbour, M., Bedward, M., Bolker, B., Borcard, D., Borman, T., Carvalho, G., Chirico, M., De Caceres, M., Durand, S., Evangelista, H. B. A., FitzJohn, R., Friendly, M., Furneaux, B., Hannigan, G., Hill, M. O., Lahti, L., Martino, C., McGlinn, D., Ouellette, M.-H., Ribeiro Cunha, E., Smith, T., Stier, A., Ter Braak, C. J. F., and Weedon, J.: *vegan: Community Ecology Package (Version 2.8-0)*, <https://doi.org/10.32614/CRAN.package.vegan>, 6 September 2025.
- Onac, B. P., Wynn, J. G., and Sumrall, J. B.: Tracing the sources of cave sulfates: A unique case from Cerna Valley, Romania, *Chem. Geol.*, 288, <https://doi.org/10.1016/j.chemgeo.2011.07.006>, 2011.
- Osenbrück, K., Fiedler, S., Knöller, K., Weise, S. M., Sültenfuß, J., Oster, H., and Strauch, G.: Timescales and development of groundwater pollution by nitrate in drinking water wells of the Jahna-Aue, Saxonia, Germany, *Water Resour. Res.*, 42, <https://doi.org/10.1029/2006WR004977>, 2006.
- Paris, G., Sessions, A. L., Subhas, A. V., and Adkins, J. F.: MC-ICP-MS measurement of  $\delta^{34}\text{S}$  and  $\Delta^{33}\text{S}$  in small amounts of dissolved sulfate, *Chem. Geol.*, 345, <https://doi.org/10.1016/j.chemgeo.2013.02.022>, 2013.
- Perez-Molphe-Montoya, E., Küsel, K., Overholt, W. A., Will Overholt, C. A., and Schiller University Jena, F.: Redefining the phylogenetic and metabolic diversity of phylum Omnitrophota, *Environ Microbiol.*, 24, 5437–5449, <https://doi.org/10.1111/1462-2920.16170>, 2022.
- Pétré, M.-A., Rivera, A., Lefebvre, R., Hendry, M. J., and Földváry, A. J. B.: A unified hydrogeological conceptual model of the Milk River transboundary aquifer, traversing Alberta (Canada) and Montana (USA), *Hydrogeol. J.*, 24, <https://doi.org/10.1007/s10040-016-1433-8>, 2016.
- Piper, A. M.: A graphic procedure in the geochemical interpretation of water-analyses, *Eos T. Am. Geophys. Un.*, 25, <https://doi.org/10.1029/TR025i006p00914>, 1944.
- Poghosyan, L., Koch, H., Lavy, A., Frank, J., van Kessel, M. A. H. J., Jetten, M. S. M., Banfield, J. F., and Lüscher, S.: Metagenomic recovery of two distinct comammox Nitrospira from the terrestrial subsurface, *Environ. Microbiol.*, 21, 3627–3637, <https://doi.org/10.1111/1462-2920.14691>, 2019.
- Purkamo, L., Bomberg, M., Nyssönen, M., Kukkonen, I., Ahonen, L., Kietäväinen, R., and Itävaara, M.: Dissecting the deep biosphere: Retrieving authentic microbial communities from packer-isolated deep crystalline bedrock fracture zones, *FEMS Microbiol. Ecol.*, 85, 324–337, <https://doi.org/10.1111/1574-6941.12126>, 2013.
- Purkamo, L., Bomberg, M., Kietäväinen, R., Salavirta, H., Nyssönen, M., Nupponen-Puputti, M., Ahonen, L., Kukkonen, I., and Itävaara, M.: Microbial co-occurrence patterns in deep Precambrian bedrock fracture fluids, *Biogeosciences*, 13, 3091–3108, <https://doi.org/10.5194/bg-13-3091-2016>, 2016.
- Purkamo, L., Kietäväinen, R., Miettinen, H., Sohlberg, E., Kukkonen, I., Itävaara, M., and Bomberg, M.: Diversity and functionality of archaeal, bacterial and fungal communities in deep Archaean bedrock groundwater, *FEMS Microbiol. Ecol.*, 94, 1–14, <https://doi.org/10.1093/femsec/fiy116>, 2018.
- Quast, C., Pruesse, E., Yilmaz, P., Gerken, J., Schweer, T., Yarza, P., Peplies, J., and Glöckner, F. O.: The SILVA ribosomal RNA gene database project: Improved data processing and web-based tools, *Nucleic Acids Res.*, 41, D590–6, <https://doi.org/10.1093/nar/gks1219>, 2013.
- Quince, C., Lanzen, A., Davenport, R. J., and Turnbaugh, P. J.: Removing Noise From Pyrosequenced Amplicons, *BMC Bioinformatics*, 12, 38, <https://doi.org/10.1186/1471-2105-12-38>, 2011.
- R Core Team: R: A language and environment for statistical computing, R Foundation for Statistical Computing, Vienna. <https://www.R-project.org> (last access: 15 May 2026), 2024.
- Rashid, A. B.: Towards Quantifying Groundwater Resources of the Paloluoma Buried Bedrock Valley in Western Finland with Groundwater Modelling, Master of Science, University of Wa-

- terloo, <http://hdl.handle.net/10012/18222> (last access: 15 May 2026), 2022.
- Retter, A., Griebler, C., Nilsson, R. H., Haas, J., Birk, S., Breyer, E., Baltar, F., and Karwautz, C.: Metabarcoding reveals ecologically distinct fungal assemblages in river and groundwater along an Austrian alpine to lowland gradient, *FEMS Microbiol. Ecol.*, 100, 139, <https://doi.org/10.1093/FEMSEC/FIAE139>, 2024.
- Ruff, S. E., Humez, P., de Angelis, I. H., Diao, M., Nightingale, M., Cho, S., Connors, L., Kuloyo, O. O., Seltzer, A., Bowman, S., Wankel, S. D., McClain, C. N., Mayer, B., and Strous, M.: Hydrogen and dark oxygen drive microbial productivity in diverse groundwater ecosystems, *Nat. Commun.*, 14, 1–17, <https://doi.org/10.1038/s41467-023-38523-4>, 2023.
- Ruuska, E., Skyttä, P., Putkinen, N., and Valjus, T.: Contribution of bedrock structures to the bedrock surface topography and groundwater flow systems within deep glaciofluvial aquifers in Kurikka, Western Finland, *Earth Surf. Proc. Land.*, 48, 2039–2056, <https://doi.org/10.1002/ESP.5602>, 2023.
- Samborska-Goik, K. and Bottrell, S.: Bayesian modelling of sulphate isotopic composition in pristine, contaminated, and experimental environments for investigating microbial bacterial reduction, *J. Hydrol.*, 652, <https://doi.org/10.1016/j.jhydrol.2024.132662>, 2025.
- Schwab, V. F., Herrmann, M., Roth, V.-N., Gleixner, G., Lehmann, R., Pohnert, G., Trumbore, S., Küsel, K., and Totsche, K. U.: Functional diversity of microbial communities in pristine aquifers inferred by PLFA- and sequencing-based approaches, *Biogeosciences*, 14, 2697–2714, <https://doi.org/10.5194/bg-14-2697-2017>, 2017.
- Shand, P., Darbyshire, D. P. F., Love, A. J., and Edmunds, W. M.: Sr isotopes in natural waters: Applications to source characterisation and water-rock interaction in contrasting landscapes, *Appl. Geochem.*, 24, <https://doi.org/10.1016/j.apgeochem.2008.12.011>, 2009.
- Shapiro, S. D., Rowe, G., Schlosser, P., Ludin, A., and Stute, M.: Tritium-helium 3 dating under complex conditions in hydraulically stressed areas of a buried-valley aquifer, *Water Resour. Res.*, 34, 1165–1180, <https://doi.org/10.1029/97WR03322>, 1998.
- Simler, R.: Software “Diagrammes,” Laboratoire d’Hydrologie d’Avignon, Université d’Avignon et pays du Vaucluse, France, <https://terre-et-eau.univ-avignon.fr/equipements-de-terrain-et-de-laboratoire/logiciels> (last access: 16 June 2026), 2012.
- Sohlberg, E., Bomberg, M., Miettinen, H., Nyssönen, M., Salavirta, H., Vikman, M., and Itävaara, M.: Revealing the unexplored fungal communities in deep groundwater of crystalline bedrock fracture zones in Olkiluoto, Finland, *Front. Microbiol.*, 6, 1–11, <https://doi.org/10.3389/fmicb.2015.00573>, 2015.
- Sonier, D. N., Duran, N. L., and Smith, G. B.: Dechlorination of Trichlorofluoromethane (CFC-11) by Sulfate-Reducing Bacteria from an Aquifer Contaminated with Halogenated Aliphatic Compounds, *Appl. Environ. Microb.*, 60, 4567–4572, 1994.
- Stroeven, A. P., Hättestrand, C., Kleman, J., Heyman, J., Fabel, D., Fredin, O., Goodfellow, B. W., Harbor, J. M., Jansen, J. D., Olsen, L., Caffee, M. W., Fink, D., Lundqvist, J., Rosqvist, G. C., Strömberg, B., and Jansson, K. N.: Deglaciation of Fennoscandia, *Quaternary Sci. Rev.*, 147, <https://doi.org/10.1016/j.quascirev.2015.09.016>, 2016.
- Tan, S., Liu, J., Fang, Y., Hedlund, B. P., Lian, Z. H., Huang, L. Y., Li, J. T., Huang, L. N., Li, W. J., Jiang, H. C., Dong, H. L., and Shu, W. S.: Insights into ecological role of a new deltaproteobacterial order Candidatus Acidulodesulfobacterales by metagenomics and metatranscriptomics, *ISME J.*, 13, 2044–2057, <https://doi.org/10.1038/s41396-019-0415-y>, 2019.
- Sültenfuß, J., Roether, W., and Rhein, M.: The Bremen mass spectrometric facility for the measurement of helium isotopes, neon, and tritium in water, *Isot. Environ. Health. S.*, 45, <https://doi.org/10.1080/10256010902871929>, 2009.
- Suominen, S., Dombrowski, N., Sinninghe Damsté, J. S., and Villanueva, L.: A diverse uncultivated microbial community is responsible for organic matter degradation in the Black Sea sulphidic zone, *Environ. Microbiol.*, 23, 2709–2728, <https://doi.org/10.1111/1462-2920.14902>, 2021.
- Visser, A., Broers, H. P., Purtschert, R., Sültenfuß, J., and De Jonge, M.: Groundwater age distributions at a public drinking water supply well field derived from multiple age tracers ( $^{85}\text{Kr}$ ,  $^3\text{H}/^3\text{He}$ , and  $^{39}\text{Ar}$ ), *Water Resour. Res.*, 49, <https://doi.org/10.1002/2013WR014012>, 2013.
- White, T. J., Bruns, T. D., Lee, S. B., and Taylor, J. W.: Amplification and Direct Sequencing of Fungal Ribosomal RNA Genes for Phylogenetics, in: *PCR Protocols: A Guide to Methods and Applications*, Academic Press, New York, edited by: Innis, M. A., Gelfand, D. H., Sninsky, J. J., and White, T. J., 315–322, <https://doi.org/10.1016/B978-0-12-372180-8.50042-1>, 1990.
- Wickham, H.: *ggplot2: Elegant Graphics for Data Analysis*, Springer Cham, 260 p., <https://doi.org/10.1007/978-3-319-24277-4>, 2016.
- Wickham, H., François, R., Henry, L., Müller, K., and Vaughan, D.: *dplyr: A Grammar of Data Manipulation (Version 1.2.0)*, <https://dplyr.tidyverse.org> (last access: 12 February 2026), 2026.
- Wilke, C. O.: *cowplot: Streamlined Plot Theme and Plot Annotations for “ggplot2”*. R package version 1.2.0, <https://wilkelab.org/cowplot/> (last access: 31 March 2025), 2025.
- Williams, T. J., Allen, M. A., Berengut, J. F., and Cavicchioli, R.: Shedding Light on Microbial “Dark Matter”: Insights Into Novel Cloacimonadota and Omnitrophota From an Antarctic Lake, *Front. Microbiol.*, 12, 741077, <https://doi.org/10.3389/fmicb.2021.741077>, 2021.
- Yilmaz, P., Parfrey, L. W., Yarza, P., Gerken, J., Pruesse, E., Quast, C., Schweer, T., Peplies, J., Ludwig, W., and Glöckner, F. O.: The SILVA and “All-species Living Tree Project (LTP)” taxonomic frameworks, *Nucleic Acids Res.*, 42, D643–D648, <https://doi.org/10.1093/nar/gkt1209>, 2014.
- Yu, T. L., Wang, B. S., Shen, C. C., Wang, P. L., Yang, T. F., Burr, G. S., and Chen, Y. G.: Improved analytical techniques of sulfur isotopic composition in nanomole quantities by MC-ICP-MS, *Anal. Chim. Acta*, 988, <https://doi.org/10.1016/j.aca.2017.08.012>, 2017.
- Zhang, J., Shi, Q., Fan, S., Zhang, Y., Zhang, M., and Zhang, J.: Distinction between Cr and other heavy-metal-resistant bacteria involved in C/N cycling in contaminated soils of copper producing sites, *J. Hazard. Mater.*, 402, 123454, <https://doi.org/10.1016/J.JHAZMAT.2020.123454>, 2021.